Mathematical Problems in Engineering

Fault Ride-Through Enhancement for Converter-Based Renewable Energy Sources

Lead Guest Editor: Mojtaba Nasiri
Guest Editors: Afef Fekih and Meisam Farrokhifar

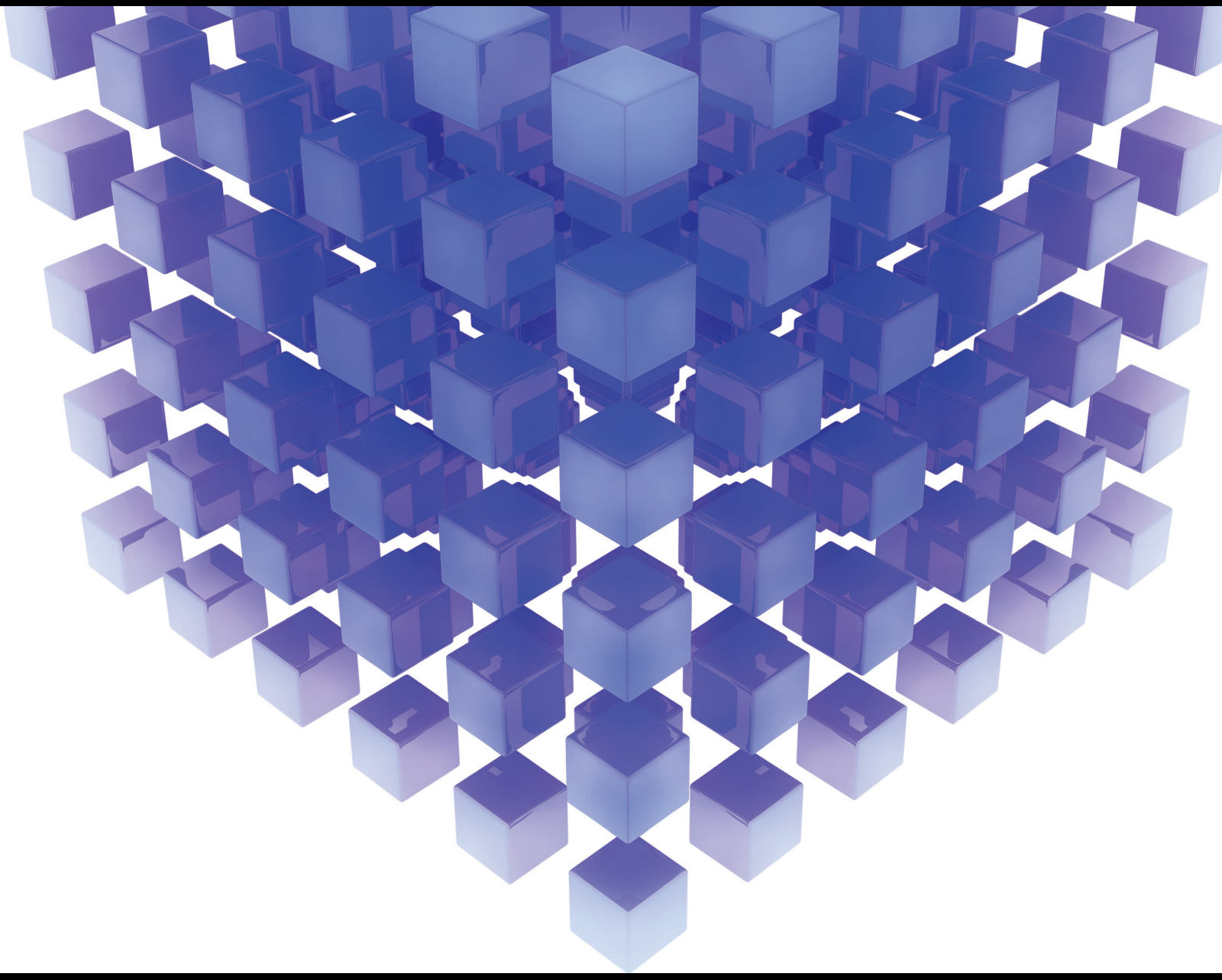

Fault Ride-Through Enhancement for Converter-Based Renewable Energy Sources

Mathematical Problems in Engineering

Fault Ride-Through Enhancement for Converter-Based Renewable Energy Sources

Lead Guest Editor: Mojtaba Nasiri
Guest Editors: Afef Fekih and Meisam Farrokhifar

Contents

Hindawi
Mathematical Problems in Engineering
Volume 2021, Article ID 9999918, 16 pages
https://doi.org/10.1155/2021/9999918

Research Article

Diagnosis and Fault-Tolerant Control of Six-Phase Wind Turbine under Multiple Open-Switch Faults

Rouhollah Bolbolnia,[1] **Karim Abbaszadeh**,[1] **and Mojtaba Nasiri**[2]

[1]*Department of Electrical and Computer Engineering, K. N. Toosi University of Technology, Tehran, Iran*
[2]*Solar Energy Applications Group, School of Engineering, Trinity College Dublin, Dublin 2, Ireland*

Correspondence should be addressed to Rouhollah Bolbolnia; r.bolbolnia@email.kntu.ac.ir

Received 30 March 2021; Revised 18 July 2021; Accepted 20 September 2021; Published 7 October 2021

Academic Editor: Adrian Neagu

A new open-switch fault diagnosis method is proposed in this paper for the six-phase AC-DC converter based on the difference between the phase current and the corresponding reference using an adaptive threshold. The single and multiple open-switch faults are detected without any additional equipment and complicated calculations since the proposed fault detection method is integrated with the hysteresis controller. The proposed fault-tolerant technique reduces the value of overcurrent and total harmonic distortion on the side phases of the faulty one, by changing the switching signal of one switch in its opposite phase in some regions. This technique is performed without adding any legs, switches, or triode for alternating currents to the circuit. Finally, the proposed fault-tolerant technique is evaluated by MATLAB simulation and the results show its effectiveness.

1. Introduction

Recently, due to the rapid growth of wind energy and its significant effect on the power grid, the reliability and availability of wind energy systems have become very important [1]. A wind turbine with a permanent magnet synchronous generator (PMSG) has the advantages of high density and efficiency and increased reliability due to the absence of gearboxes [2]. These benefits alleviate the investment concerns in a PMSG wind turbine [3]. On the other hand, using multiphase generators in wind turbine systems provides more advantages such as reducing the amplitude of pulsating torque and increasing its frequency, decreasing the stator copper loss, and lowering the current per-phase for the same rated voltage. Moreover, multiphase generators improve reliability and increase the degree of freedom [4]. Therefore, a six-phase PMSG is one of the best choices for a wind turbine system. A wind turbine equipped with a six-phase PMSG requires a full-scale converter to inject the desired power into the grid. According to recent studies [5], the most vulnerable components of a wind turbine system are its power electronics devices and the most faults are originated from power switches, resulting in 25% of failures. Another survey [6] shows that power electronic converters are responsible for more than 22% of the overall downtimes in wind farms, which is the longest one of all. Generally, power switch faults are categorized into two types of short-circuit and open-switch faults. Unlike the short-circuit fault, the open-switch fault does not cause the system to immediately shut down and can remain undetected for a while [7]. However, it can disrupt the performance and reliability of the system, lead to secondary faults in the converter, eventually resulting in complete shutdown of the system [8, 9]. In order to improve the reliability and availability levels and reduce maintenance costs, both diagnostic and fault-tolerant methods with acceptable performance are needed until the situation is revised [10, 11].

In general, diagnostic methods can be categorized into the following three groups: model-based, knowledge-based, and signal-based. By employing an observer in [12, 13], a model-based fault diagnostic approach was implemented. However, the model-based methods require accurate information of the system model and are extremely sensitive to the system parameter variations [7]. In [14], a knowledge-based fuzzy fault diagnosis method for the voltage source inverters was proposed. Nevertheless, the knowledge-based

methods need the historic data of the system and require long training and a huge computational effort. The signal-based methods are realized by examining the characteristics of voltage and current signals. A single open-switch fault diagnostic method based on a comparison between the measured voltage and the reference value was presented for a doubly fed wind power system in [1, 15]. Voltage-based diagnostic methods increase the system cost, complexity, and the potential of fault on additional equipment like voltage sensors [16]. Current-based methods are widely used for single and multiple open-switch fault detection since they require neither accurate model of the system, complicated calculations, nor additional equipment [10]. The current Park's vector and the average current Park's vector methods were introduced in [17, 18], whereas the open-switch fault was determined by using the phase angle. A comparison between the phase angle slope of the current Park's vector and a constant threshold was suggested in [19, 20]. The fault diagnosis indicator is normalized to be independent of load changes. In [21, 22], the fundamental component and the average absolute value of the current were considered as normalizing variables. In [23], the instantaneous value of the current was proposed as a normalizing variable. The constant thresholds usually need to be adjusted according to the operating point variation or reference values, which can decrease the reliability of fault diagnosis techniques [24]. In [25], the adaptive threshold is used instead of the constant threshold to increase robustness. These techniques detect open-switch faults in conventional three-phase converters with six switches but they have not been analyzed for multiphase systems, yet.

Various structures were proposed for open-switch fault-tolerant. In [26, 27], an additional leg was connected to the converter phases by triode for alternating currents (TRIACs), while in [28], this additional leg was connected to the neutral point of the machine. Besides, in [29] and [30], the additional switches were removed, and only by TRIACs, the capacitors midpoint of DC-link was connected to the converter phases or the neutral point of the machine or grid transformer [31, 32]. Also in [33], both sides (grid/machine) of the back-to-back converter were connected to each other through TRIACs. Additional equipment such as switches and TRIACs increases the cost and complexity of the system. In some researches [8, 34, 35], the fault-tolerant method was implemented by revising the PWM switching pattern, which prevents the system cost to increase. Also, these methods have not been evaluated for multiphase systems.

This paper presents a fault diagnosis technique for single and multiple open-switch faults in a six-phase AC-DC converter as part of a multiphase wind turbine system. The novelties of this paper can be classified as follows:

(1) The proposed fault detection method only requires the information given by current sensors and their reference signals

(2) These currents and their reference information are already provided by the main control system and there is no need for additional sensors or complicated calculations

(3) After fault detection, without any additional equipment, the fault-tolerant method is performed by revising the switching pattern of the opposite phase of the faulty ones in some regions

(4) The proposed fault-tolerant method reduces the overcurrent and the total harmonic distortion (THD) of current in healthy phases

This paper is arranged as follows: The six-phase AC-DC converter model used in the wind turbine is presented in Section 2. Fault detection technique and fault-tolerant method for single and multiple open-switch faults are introduced in Section 3 and Section 4, respectively. In Section 5, the performance of the proposed fault-tolerant method is evaluated by utilizing simulation results. Finally, in Section 6, conclusions are presented.

2. Description of the Six-Phase Wind Turbine with the AC-DC Converter Model

A wind turbine based on a six-phase PMSG is connected to the grid via a full-scale back-to-back converter. According to Figure 1, this converter consists of two parts, machine side converter (MSC) and grid side converter (GSC), which are connected to each other through the DC-link capacitor. As the six-phase MSC has 12 switches (twice the three-phase system), open-switch fault diagnosis and fault-tolerant are very important in this converter. Many fault detection and fault-tolerant methods have been developed for DC-AC inverter; however, there are a few types of research for AC-DC converter [8]. This paper uses a six-phase AC-DC converter without grid connection and considers a local load as a consumer according to Figure 2.

Figure 3 demonstrates a hysteresis current controller in a six-phase AC-DC converter to maintain the DC-link voltage at the required value. The main advantage of the hysteresis controller is its simplicity, fast response, and load-independent performance [36]. A proportional integral (PI) controller is used to regulate the DC-link voltage and its reference value [37]. The output of the DC-link voltage controller is considered as the reference current I_{ref} in the hysteresis controller. The reference current waveform is obtained from the voltage waveform of the same phase. Switching signals for each phase are generated by comparing the phase current with its reference value and considering the hysteresis band. If the difference between the reference current and the actual current of the same phase is greater than the hysteresis band, the upper switch of that phase will turn on. Otherwise, the bottom switch of that phase will turn on. The differential equation of the six-phase AC-DC converter is given by

$$u_{sn}(t) = L\frac{\mathrm{d}i_{sn}}{\mathrm{d}t} + Ri_{sn}(t) + u_{\mathrm{mod}-n}(t) \quad n = a, b, c, x, y, z, \tag{1}$$

where u_s is the voltage source and u_{mod} is the converter voltage. L is the filter's inductance, and R is the resistance. The six-phase converter equations are transferred to the dq rotation frame by considering the T_{62} matrix.

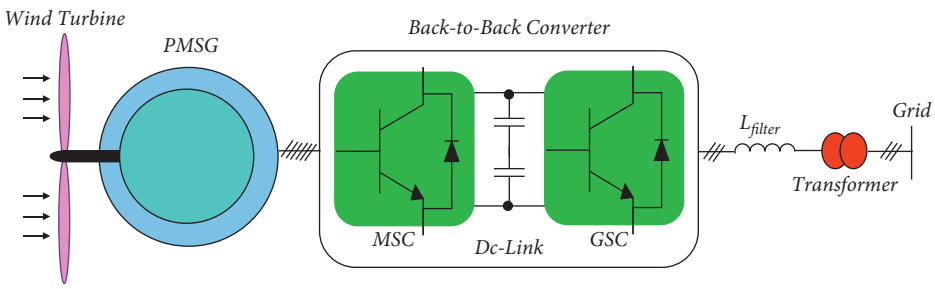

Figure 1: The six-phase PMSG-based wind turbine system configuration.

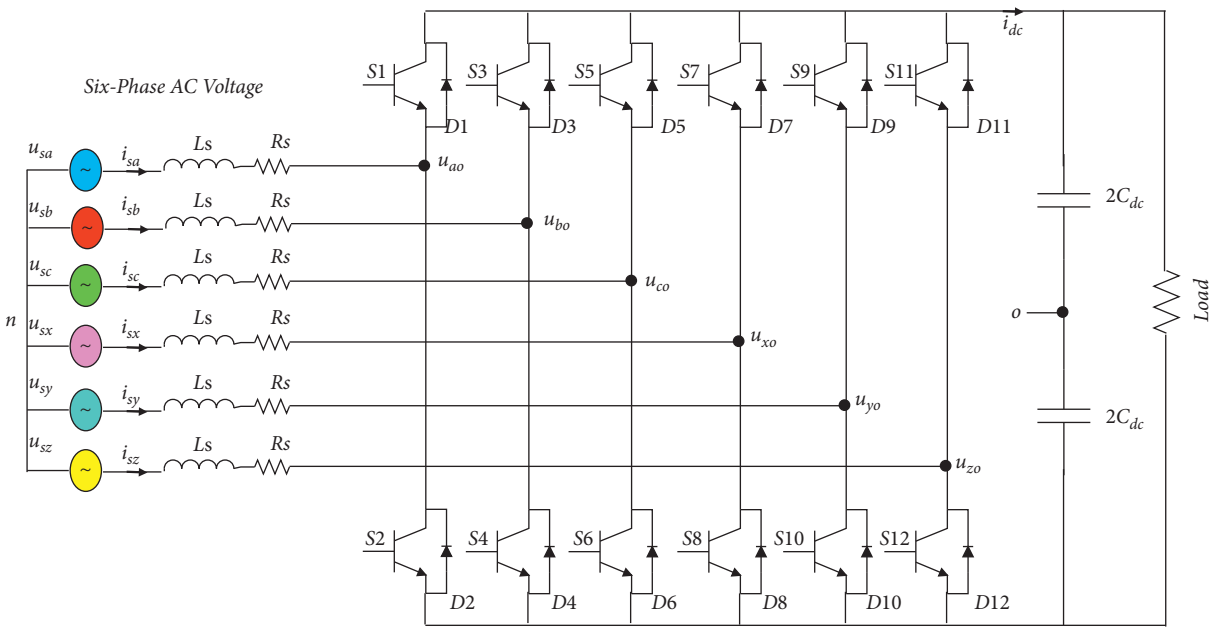

Figure 2: Six-phase AC-DC PWM converter.

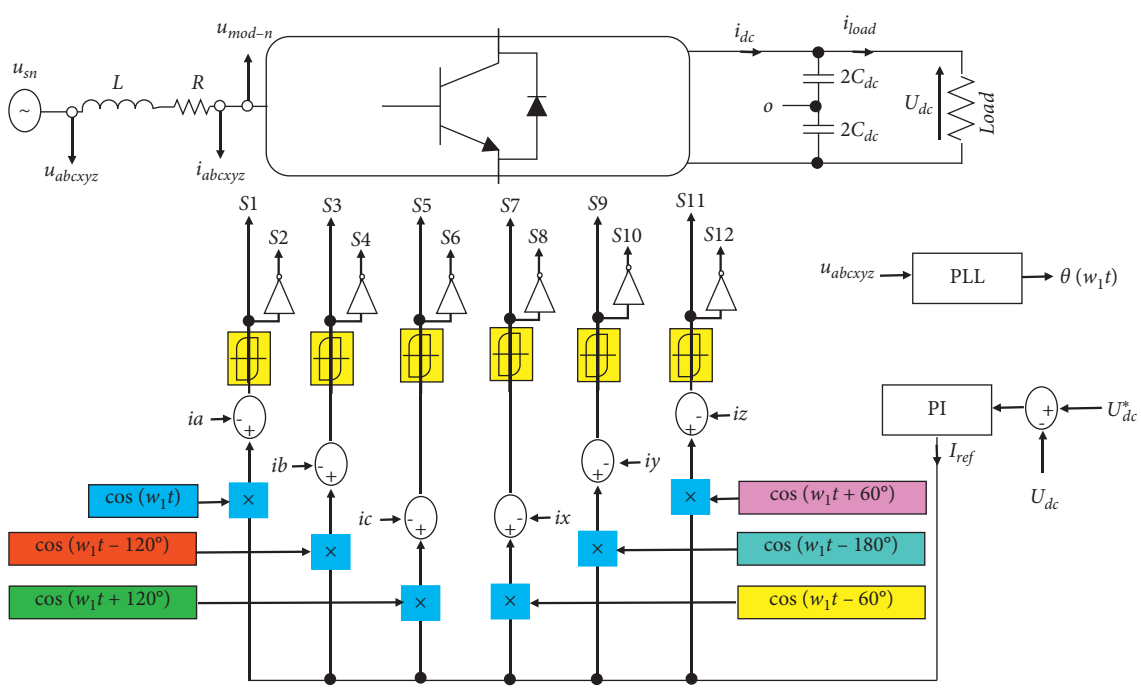

Figure 3: Control block diagram of direct current control utilizing hysteresis controller in a six-phase AC-DC converter.

$$T_{62} = \frac{2}{6}\begin{bmatrix} \cos(\theta) & \cos\left(\theta - \frac{2\pi}{3}\right) & \cos\left(\theta + \frac{2\pi}{3}\right) & \cos\left(\theta - \frac{\pi}{3}\right) & \cos(\theta - \pi) & \cos\left(\theta + \frac{\pi}{3}\right) \\ -\sin(\theta) & -\sin\left(\theta - \frac{2\pi}{3}\right) & -\sin\left(\theta + \frac{2\pi}{3}\right) & -\sin\left(\theta - \frac{\pi}{3}\right) & -\sin(\theta - \pi) & -\sin\left(\theta + \frac{\pi}{3}\right) \end{bmatrix},$$

$$\frac{d}{dt}\begin{bmatrix} id(t) \\ iq(t) \end{bmatrix} = \begin{bmatrix} -\frac{R}{L} & w_1 \\ -w_1 & -\frac{R}{L} \end{bmatrix}\begin{bmatrix} id(t) \\ iq(t) \end{bmatrix} + \begin{bmatrix} -\frac{1}{L} & 0 \\ 0 & -\frac{1}{L} \end{bmatrix}\begin{bmatrix} u_{\mathrm{mod},d}(t) \\ u_{\mathrm{mod},q}(t) \end{bmatrix} + \begin{bmatrix} \frac{1}{L} & 0 \\ 0 & \frac{1}{L} \end{bmatrix}\begin{bmatrix} u_{s,d}(t) \\ u_{s,q}(t) \end{bmatrix}, \tag{2}$$

where w_1 is the angular frequency and i_d and i_q are d-axis and q-axis currents, respectively. u_{sd} and u_{sq} are d-axis and q-axis voltages, respectively. Source power (P_s) is considered based on equation (3). A part of the source power is dissipated as losses in the converter (P_{losses}) and the rest is delivered to the load (P_{load}).

$$P_s = P_{load} + P_{losses} = 3\left(u_{s,d}.i_d + u_{s,q}.i_q\right). \tag{3}$$

3. Diagnosis of Open-Switch Faults

The open-switch faults in the six-phase AC-DC PWM converters have different current patterns compared to the six-phase voltage source inverters. Unlike inverters, these converters do not completely block positive and negative currents during open-switch faults. As shown in Figure 2, in normal operation, the positive half-cycle current is established through the bottom switch and the upper antiparallel diode of one phase, whereas the upper switch and the bottom antiparallel diode of that phase establish the negative half-cycle current. Therefore, if an open-switch fault occurs on the upper switch, the negative half-cycle of phase current is distorted but its positive half-cycle is not affected. On the contrary, if an open-switch fault occurs in the bottom switch, the negative half-cycle of phase current is not affected but its positive half-cycle is distorted. Hence, the open-switch faults can be detected by monitoring the lost part of the phase current [32].

Open-switch faults include single and multiple faults. Two different cases are considered for the multiple open-switch faults:

Case I: the open-switch fault occurs in two switches from two different legs

Case II: the open-switch fault occurs in two switches from one leg

3.1. Single Open-Switch Fault. Due to the open-switch fault that occurred in the upper or bottom switch, part of the negative or positive half-cycle current of that leg is eliminated, which is different from its corresponding reference signal. Therefore, the difference between the phase current and the corresponding reference is used as a fault diagnosis indicator. This fault diagnosis indicator does not require additional measurements so it is integrated with the control block diagram of converter, as shown in Figure 3. The fault diagnosis indicator is normalized to be independent of the load [38].

The first fault diagnosis indicator is normalized residual current Nr_n. As shown in (4), Nr_n is the average value of the absolute current error divided by the absolute current value. in and in^* are the current and its reference value of each phase, respectively. δ is a small positive quantity.

$$\mathrm{Nr}_n = \left\langle \frac{\left|i_n - i_n^*\right|}{\delta + \left|i_n\right|} \right\rangle \quad n = a, b, c, x, y, z. \tag{4}$$

In normal conditions, the value of Nr_n is approximately equal to zero in all phases. When the fault occurs, Nr_n of the corresponding phase will change and exceed the threshold value. A good threshold value is essential for a robust fault diagnosis [38]. If the fixed threshold value is high or low, then the fault sensitivity is reduced or the false alarm rate is increased, respectively. Therefore, an adaptive threshold value is the best alternative. According to equation (6), the adaptive threshold value is the average of $R_{\max}$ and $R_{\min}$. In this equation, $R_{\max}$ is the maximum of Nr_n in all phases, and R_{min} is the minimum of Nr_n in all phases.

$$T = \frac{R_{\max} + R_{\min}}{2},$$
$$R_{\max} = \max\left\{\mathrm{Nr}_a, \mathrm{Nr}_b, \mathrm{Nr}_c, \mathrm{Nr}_x, \mathrm{Nr}_y, \mathrm{Nr}_z\right\}, \tag{5}$$
$$R_{\min} = \min\left\{\mathrm{Nr}_a, \mathrm{Nr}_b, \mathrm{Nr}_c, \mathrm{Nr}_x, \mathrm{Nr}_y, \mathrm{Nr}_z\right\}.$$

Under normal conditions, the adaptive threshold value is similar to the value of Nr_n, which is approximately equal to zero. Nevertheless, in fault conditions, due to a sudden change in the value of Nr_n, the value of $R_{\max}$ increases. As a result, the adaptive threshold value also increases and becomes greater than zero [35]. Since T is the average value of $R_{\max}$ and $R_{\min}$, so it is smaller than Nr_n in the faulty phase. Moreover, as Nr_n has not changed in other phases, their value has become less than T. The phase with the single open-switch fault is detected by considering the first fault diagnosis indicator (Nr_n) and the adaptive threshold value (T) according to Table 1.

Table 1: The different states of the single open-switch fault diagnosis.

Normal condition	$\mathrm{Nr}_a \approx T$	$\mathrm{Nr}_b \approx T$	$\mathrm{Nr}_c \approx T$	$\mathrm{Nr}_x \approx T$	$\mathrm{Nr}_y \approx T$	$\mathrm{Nr}_z \approx T$
Fault in phase a	$Nr_a > T$	$\mathrm{Nr}_b < T$	$\mathrm{Nr}_c < T$	$\mathrm{Nr}_x < T$	$\mathrm{Nr}_y < T$	$\mathrm{Nr}_z < T$
Fault in phase b	$\mathrm{Nr}_a < T$	$\mathrm{Nr}_b > T$	$\mathrm{Nr}_c < T$	$\mathrm{Nr}_x < T$	$\mathrm{Nr}_y < T$	$\mathrm{Nr}_z < T$
Fault in phase c	$\mathrm{Nr}_a < T$	$\mathrm{Nr}_b < T$	$\mathrm{Nr}_c > T$	$\mathrm{Nr}_x < T$	$\mathrm{Nr}_y < T$	$\mathrm{Nr}_z < T$
Fault in phase x	$\mathrm{Nr}_a < T$	$\mathrm{Nr}_b < T$	$\mathrm{Nr}_c < T$	$\mathrm{Nr}_x > T$	$\mathrm{Nr}_y < T$	$\mathrm{Nr}_z < T$
Fault in phase y	$\mathrm{Nr}_a < T$	$\mathrm{Nr}_b < T$	$\mathrm{Nr}_c < T$	$\mathrm{Nr}_x < T$	$\mathrm{Nr}_y > T$	$\mathrm{Nr}_z < T$
Fault in phase z	$\mathrm{Nr}_a < T$	$\mathrm{Nr}_b < T$	$\mathrm{Nr}_c < T$	$\mathrm{Nr}_x < T$	$\mathrm{Nr}_y < T$	$\mathrm{Nr}_z > T$

As shown in Figure 2, each phase has two switches. After detecting the faulty phase, it is necessary to determine whether the open-switch fault occurred in the upper switch or the bottom one. Therefore, the average current value $<in>$ is considered as another indicator of open-switch fault diagnosis to distinguish between the upper and bottom switch. If the value of $<in>$ is higher than zero, the open-switch fault has occurred in the upper switch. Hence, the open-switch fault has occurred in the bottom switch when $<in>$ is lower than zero. The block diagram of the open-switch fault based on the two indicators Nr_n and $<in>$ is presented in Figure 4.

3.2. Multiple Open-Switch Faults. Multiple open-switch faults occur in at least two switches of one leg or two different legs. The value of Nr_n in the faulty phases is greater than the adaptive threshold while it is smaller in healthy phases. For example in Figure 2, if S_2 and S_{11} are in a faulty state, i_a and i_z will lose their positive and negative half-cycles, respectively. Accordingly, Nr_a and Nr_z are greater than T whereas Nr_b, Nr_c, Nr_x , and Nr_y are smaller than T. Similar to the single open-switch fault, the average current value is used to discern the upper switch from the bottom switch in multiple open-switch fault modes. Therefore, $<i_a>$ is smaller than zero because S_2 is the bottom switch and $<i_z>$ is larger than zero because S_{11} is the upper switch.

When multiple open-switch faults occur in the upper and the bottom switches from one leg, only the value of Nr_n in that phase is greater than the adaptive threshold, similar to the single open-switch fault. In this case, the average current value is used to distinguish between single and multiple open-switch faults of a leg. In a single open-switch fault condition, the value of $<i_n>$ in the faulty phase is greater than zero or smaller than zero, while in multiple open-switch faults on both switches of one leg, the value of $<i_n>$ becomes approximately equal to zero after a considerable fluctuation.

4. The Proposed Fault-Tolerant Method for Open-Switch Faults

Open-switch faults in the six-phase converters do not immediately cause the system to shut down, but they compromise the performance of the converters. To improve the converter's performance and prevent secondary fault, the fault-tolerant control takes place. Figure 5 shows the six-phase currents of the AC-DC converter in the normal operation, which is similar to the voltage waveform due to the unity power factor. The general equation of the current is as follows:

$$\mathrm{i}_k = I_m \cos\left(w_1 t - \frac{(k-1)*\pi}{3}\right) \quad k = 1, 2, \ldots 6, \tag{6}$$

where Im is the six-phase current amplitude and w_1 is the angular frequency. Every cycle of the currents can be divided into 12 regions, where their corresponding devices with normal operation are presented in Table 2. According to Table 2, under normal conditions in each region, three of the upper switches of each phase and three of the bottom switches of the other phases conduct currents.

According to Kirchhoff's circuit laws, the sum of the six-phase currents should be zero. Since the faulty switch is unable to conduct its corresponding half-cycle current, this current is imposed to the side phases, thus causing an overcurrent. For each side phase, the overcurrent can be calculated by

$$i_{fault\,(k-1)} = I_m \cos\left(w_1 t - \frac{(k-2)*\pi}{3}\right) + I_m \cos\left(w_1 t - \frac{(k-1)*\pi}{3}\right) = \sqrt{3} * I_m \cos\left(w_1 t - \frac{(k-2)\pi}{3} + \frac{\pi}{6}\right), \tag{7}$$

$$i_{fault\,(k+1)} = I_m \cos\left(w_1 t - \frac{k\pi}{3}\right) + I_m \cos\left(w_1 t - \frac{(k-1)*\pi}{3}\right) = \sqrt{3} * I_m \cos\left(w_1 t - \frac{k\pi}{3} + \frac{\pi}{6}\right), \tag{8}$$

where k is the faulty phase and *ifault* is the fault current. Therefore, the amplitude of the overcurrent is more than 73% of the rated phase current, which causes terrible stresses on the switches of these phases. Accordingly, there is a high possibility of secondary faults in the converter system, and the proposed fault-tolerant control should limit this overcurrent in other healthy phases.

4.1. Fault-Tolerant Method for a Single Open-Switch Fault. According to Figure 5 and equation (6), the currents of phases A, B, and C are symmetrical with the currents of phases Y, Z, and X, respectively. In other words, phase Y is the opposite phase of phase A, phase Z is the opposite phase of phase B, and phase X is the opposite phase of phase C. Then, the overcurrent in healthy phases can be limited by turning off the

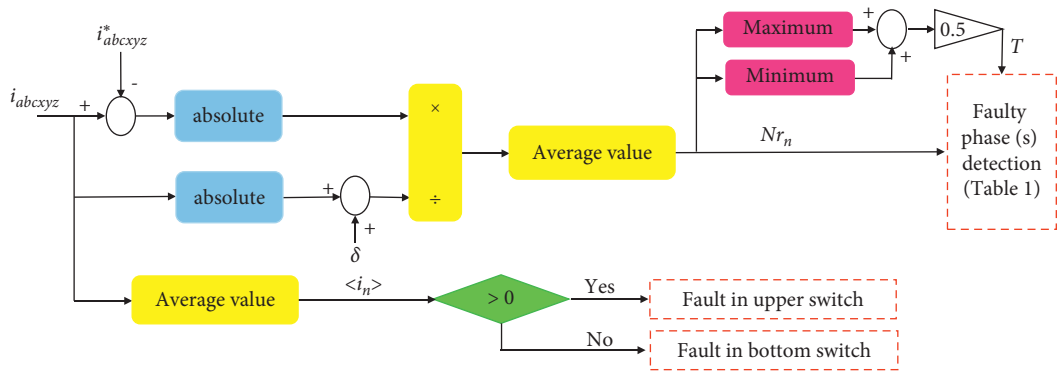

Figure 4: Block diagram of the open-switch fault detection method.

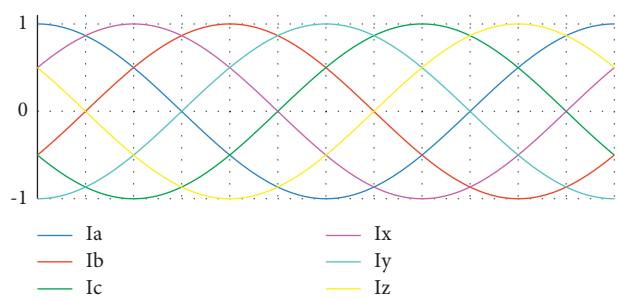

Figure 5: Six-phase currents of AC-DC converter at normal operation.

Table 2: Conducting diodes and switches of the six-phase converter at normal operation.

Regions	Conducting switches	Conducting diodes
Reg1: $(0-\frac{\pi}{6})$	$S_2, S_3, S_5, S_8, S_9, S_{12}$	$D_1, D_4, D_6, D_7, D_{10}, D_{11}$
Reg2: $(\frac{\pi}{6}-\frac{2\pi}{6})$	$S_2, S_4, S_5, S_8, S_9, S_{11}$	$D_1, D_3, D_6, D_7, D_{10}, D_{12}$
Reg3: $(\frac{2\pi}{6}-\frac{\pi}{2})$	$S_2, S_4, S_5, S_8, S_9, S_{11}$	$D_1, D_3, D_6, D_7, D_{10}, D_{12}$
Reg4: $(\frac{\pi}{2}-\frac{4\pi}{6})$	$S_1, S_4, S_5, S_8, S_{10}, S_{11}$	$D_2, D_3, D_6, D_7, D_9, D_{12}$
Reg5: $(\frac{4\pi}{6}-\frac{5\pi}{6})$	$S_1, S_4, S_5, S_8, S_{10}, S_{11}$	$D_2, D_3, D_6, D_7, D_9, D_{12}$
Reg6: $(\frac{5\pi}{6}-\pi)$	$S_1, S_4, S_6, S_7, S_{10}, S_{11}$	$D_2, D_3, D_5, D_8, D_9, D_{12}$
Reg7: $(\pi-\frac{7\pi}{6})$	$S_1, S_4, S_6, S_7, S_{10}, S_{11}$	$D_2, D_3, D_5, D_8, D_9, D_{12}$
Reg8: $(\frac{7\pi}{6}-\frac{8\pi}{6})$	$S_1, S_3, S_6, S_7, S_{10}, S_{12}$	$D_2, D_4, D_5, D_8, D_9, D_{11}$
Reg9: $(\frac{8\pi}{6}-\frac{3\pi}{2})$	$S_1, S_3, S_6, S_7, S_{10}, S_{12}$	$D_2, D_4, D_5, D_8, D_9, D_{11}$
Reg10: $(\frac{3\pi}{2}-\frac{10\pi}{6})$	$S_2, S_3, S_6, S_7, S_9, S_{12}$	$D_1, D_4, D_5, D_8, D_{10}, D_{11}$
Reg11: $(\frac{10\pi}{6}-\frac{11\pi}{6})$	$S_2, S_3, S_6, S_7, S_9, S_{12}$	$D_1, D_4, D_5, D_8, D_{10}, D_{11}$
Reg12: $(\frac{11\pi}{6}-2\pi)$	$S_2, S_3, S_5, S_8, S_9, S_{12}$	$D_1, D_4, D_6, D_7, D_{10}, D_{11}$

switches in the opposite phase of the faulty ones, in some regions. The fault-tolerant switch and fault-tolerant regions for every single open-switch fault are described in Table 3. For example, in Figure 2, if an open-switch fault occurs on the S_{11} switch, the negative half-cycle current of phase Z does not pass through this switch and causes overcurrent in phases A and C. According to Table 3, the S_4 switch in the opposite phase of phase Z must be turned off in regions 2, 3, 6, and 7 to reduce the overcurrent in healthy phases A and C.

4.2. Fault-Tolerant Method for Multiple Open-Switch Faults. After fault detection and localization in multiple open-switch faults, the proposed fault-tolerant control for both faulty switches is simultaneously performed according to Table 3. The open-switch fault of switches S_1 and S_{12} in Figure 2 is considered as an example. These multiple open-switch faults cause overcurrent in the negative half-cycle current of phases X and Z and the positive half-cycle current of phases A and C. The overcurrent in healthy phases is limited by turning off S_{10} in regions 4, 5, 8, and 9 and simultaneously S_3 in regions 1, 8, 9, and 12. To evaluate the effectiveness of the proposed fault-tolerant method, an overcurrent indicator (I_{ov}) in the side phases of the faulty one is defined according to equation (9). This method tries to reduce it.

$$I_{ov(k\pm1)} = \max \frac{\left| i_{fault(k\pm1)} - i_{normal(k\pm1)} \right|}{\left| i_{normal(k\pm1)} \right|}, \tag{9}$$

where k is the faulty phase and $k \pm 1$ are the side phases. *ifault* and *inormal* are the phase current in faulty and healthy conditions.

Table 3: Fault-tolerant switch and fault-tolerant regions for six-phase AC-DC converter at open-switch fault conditions.

Open-switch fault	Fault-tolerant switch	Fault-tolerant regions
S_1	S_{10}	Reg4, Reg5, Reg8, Reg9
S_2	S_9	Reg2, Reg3, Reg10, Reg11
S_3	S_{12}	Reg1, Reg8, Reg9, Reg12
S_4	S_{11}	Reg2, Reg3, Reg6, Reg7
S_5	S_8	Reg1, Reg4, Reg5, Reg12
S_6	S_7	Reg6, Reg7, Reg10, Reg11
S_7	S_6	Reg6, Reg7, Reg10, Reg11
S_8	S_5	Reg1, Reg4, Reg5, Reg12
S_9	S_2	Reg2, Reg3, Reg10, Reg11
S_{10}	S_1	Reg4, Reg5, Reg8, Reg9
S_{11}	S_4	Reg2, Reg3, Reg6, Reg7
S_{12}	S_3	Reg1, Reg8, Reg9, Reg12

5. Simulation Results

To evaluate the performances of the proposed fault detection method and fault-tolerant control in the six-phase AC-DC converter, several simulations are carried out by using the MATLAB/Simulink software. The simulation parameters and open-switch fault conditions are given in Table 4. Although the fault-tolerant technique can be performed immediately after fault detection, it is performed after a while (at $t = 0.3$ s) to make its effect more clear. The simulation results are divided into three-time intervals:

(1) Normal condition: $t < 0.2$ s

(2) Open-switch fault time: $0.2\text{ s} < t < 0.3\text{ s}$

(3) Fault-tolerant time: $t > 0.3$ s

Firstly, the robustness of the fault detection method against load changes should be evaluated. According to Figure 6(a), assume that the load connected to the converter is halved at $t = 0.14$ s. As shown in Figure 6(b), the load changes affect all the phases and increase the value of Nr_n and T, but they stay close to each other. Therefore, the fault detection method correctly identifies such changes as nonfault conditions and it is robust against them.

According to Figure 7(a), an open-switch fault has occurred in the switch *S11* in at the moment $t = 0.2$ s, which has caused a disturbance in the six-phase currents. Part of the negative half-cycle current of phase Z is eliminated, while phases A and C suffer 66 percent overcurrent.

Under normal conditions, the values of the actual and reference currents are close to each other, so the values of Nr_n and T are about zero. After the start time of the single open-switch fault, the values of Nr_n in the faulty phase will increase, and consequently, the value of T will increase. Since $(T > \mathrm{Nr}_a)$, $(T > \mathrm{Nr}_b)$, $(T > \mathrm{Nr}_c)$, $(T > \mathrm{Nr}_x)$, $(T > \mathrm{Nr}_y)$ and $(T < \mathrm{Nr}_z)$, the open-switch fault is detected in phase Z at $Tfd = 0.2023$ s according to Table 1 and Figure 8. As shown in Figure 9, the value of $<iz>$ is greater than zero, so the open-switch fault occurred in the upper switch of phase Z.

After identifying the faulted switch *S11*, the fault-tolerant control is executed at $t = 0.3$ s, according to Table 3. As shown in Figure 7(b), during the open-switch fault of the *S11*, the *S4* switch is turned off in regions 2, 3, 6, and 7, to reduce the overcurrent of phases A and C. By applying the fault-tolerant method, in addition to reducing the overcurrent in phases A and C, the THD of current in these phases is also reduced. The THD of phases A and C is presented in Figure 10. The numerical results of the overcurrent indicator and THD for the side phases of the faulty phase at the open-switch fault time and fault-tolerant time are presented in Table 5.

Since a fault on any switch may also cause other switches to fail, multiple switch faults are very significant and should be addressed properly. For example, consider the open-switch faults on switches *S1* and *S12* that cause an overcurrent in the negative half-cycle of phases X and Z and the positive half-cycle of phases A and C, respectively. As shown in Figure 11(a) and Table 5, the value of overcurrent will be reduced by turning off S_{10} in regions 4, 5, 8, and 9 and S_3 in regions 1, 8, 9, and 12. This reduction in the side phases A and C after implementing the fault-tolerant method is specifically shown in Figure 11(b). According to Figure 12 and Table 5, the THD of current in healthy phases is reduced by executing the fault-tolerant method.

Multiple open-switch faults occur when the value of Nr_n in more than one phase is greater than the value of T while in the other phases it is smaller than the value of T. According to Figure 13, when $(T > \mathrm{Nr}_b)$, $(T > \mathrm{Nr}_c)$, $(T > \mathrm{Nr}_x)$, $(T > \mathrm{Nr}_y)$ $(T < \mathrm{Nr}_a)$, and $(T < \mathrm{Nr}_z)$, the open-switch faults occurred in phases A and Z at $Tfd = 0.2062$ s. The value of $<ia>$ is greater than zero and the value of $<iz>$ is smaller than zero; therefore, the open-switch faults occurred in the upper switch of phase A (*S1*) and the bottom switch of phase Z (*S12*), as shown in Figure 14.

In cases where multiple open-switch faults occur in both switches of one leg, the value of Nr_n in that phase is greater than the value of T. However, unlike a single open-switch fault, the value of $<in>$ does not remain positive or negative and after a significant fluctuation becomes approximately zero again. The values Nr_n and $\langle in \rangle$ are shown in Figures 15 and 16 for multiple open-switch faults in both switches of phase A. Since only $(T < \mathrm{Nr}_a)$, the open-switch fault is detected in phase A at $Tfd = 0.203$ s, as shown in Figure 15. According to Figure 16, the value of $<ia>$ also came close to zero again at the time of fault.

In fault-tolerant time for open-switch fault in both switches of phase A, switches S_{10} and S_9 must be turned off

Table 4: Parameters of the six-phase AC-DC converter simulation.

Input voltage	6 ph-230 (v)	DC-link voltage	650 (V)	Control format	Hysteresis (s)
Grid frequency	50 (Hz)	DC-link capacitance	2200 (μF)	Fault start time	0.2
Reactor	5 (mH)	DC load resistance	100 (ohm)	Tolerant control start time	0.3

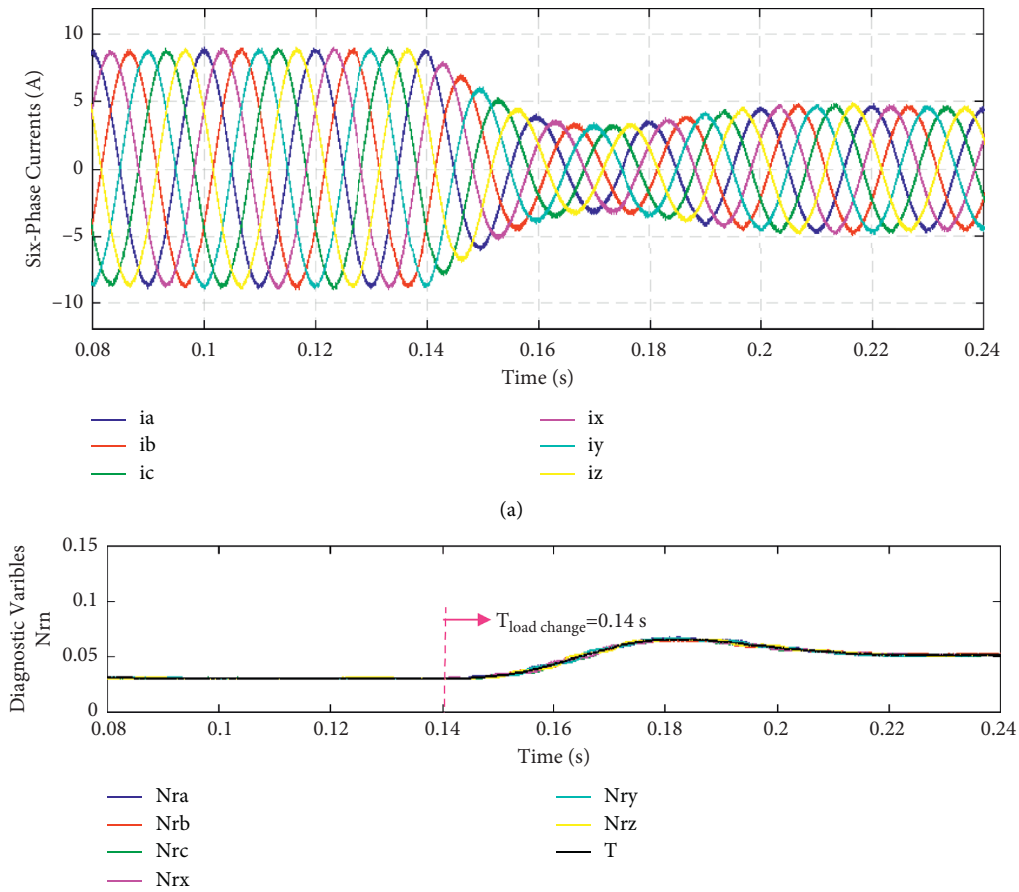

Figure 6: Simulation result to prove the robustness of the fault detection method against load changes. (a) Six-phase currents. (b) Diagnostic variables Nr_n.

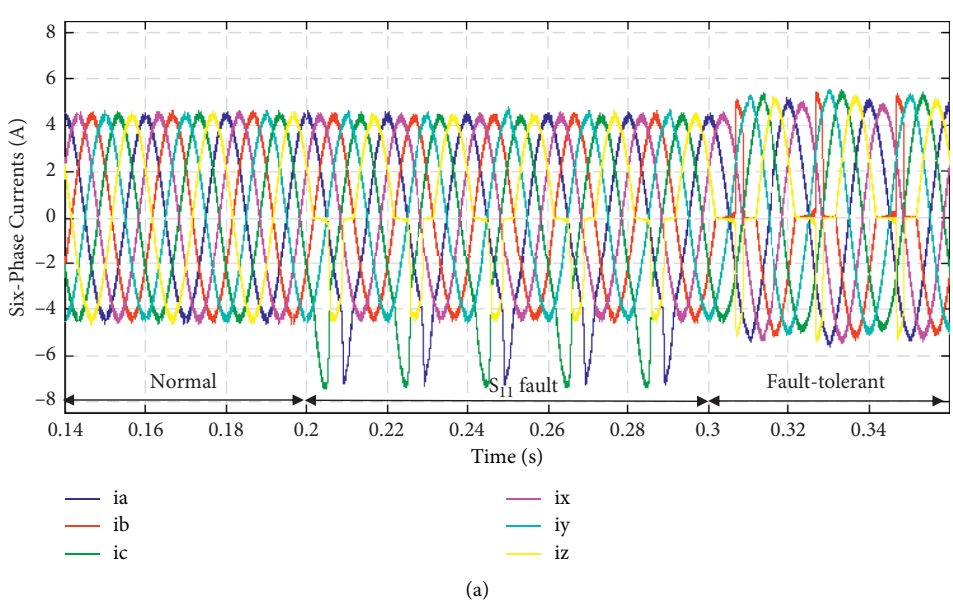

Figure 7: Continued.

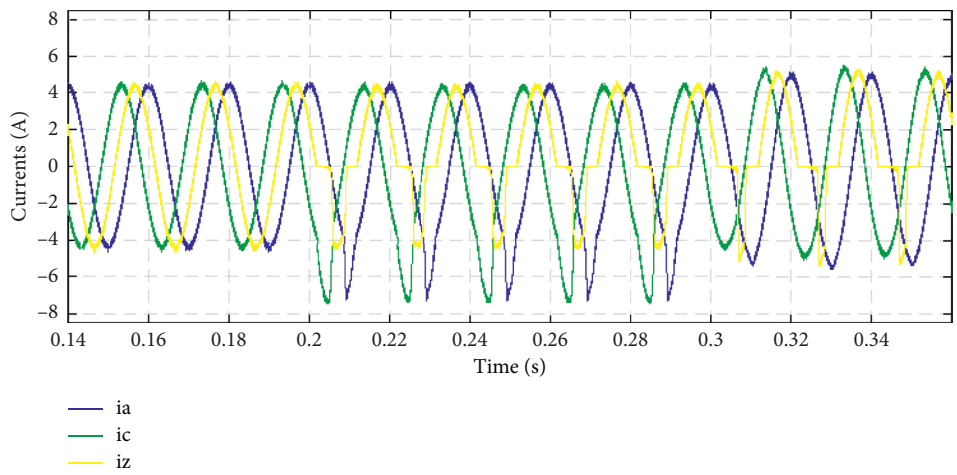

(b)

Figure 7: Simulation result of the AC-DC converter currents before and after open-switch fault in *S11*. (a) All phases. (b) Faulty phase *Z* and side phases *A* and *C*.

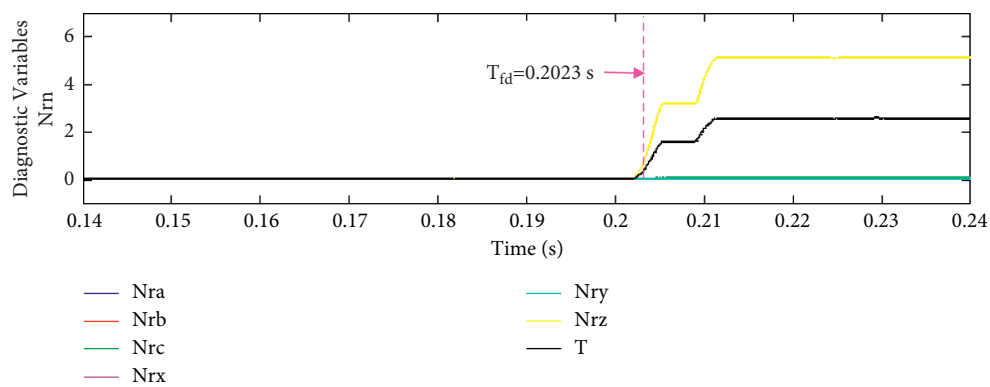

Figure 8: Simulation result of the diagnostic variables *Nrn*, for open-switch faults in phase *Z*.

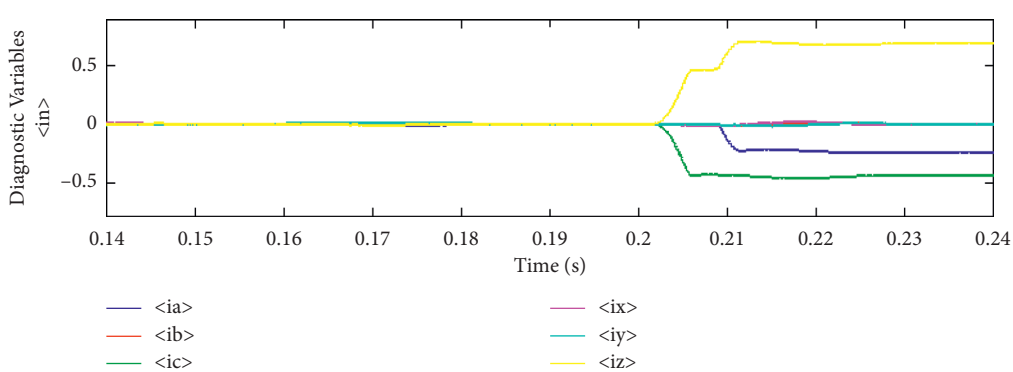

Figure 9: Simulation result of the diagnostic variables $\langle in \rangle$, for open-switch faults in S_{11}.

in regions (4, 5, 8, and 9) and (2, 3, 10, and 11), respectively. According to Figure 17, Figure 18, and Table 5, by implementing the fault-tolerant method, the value of overcurrent and THD of current in phases *X* and *Z* are reduced.

In both single and multiple open-switch faults, the maximum value of DC-link voltage ripple is 5 volts, which is smaller than 1% of the reference value. Figure 19 shows the DC-link voltage ripple for single open-switch fault, multiple open-switch faults in two legs, and both switches of one leg, respectively.

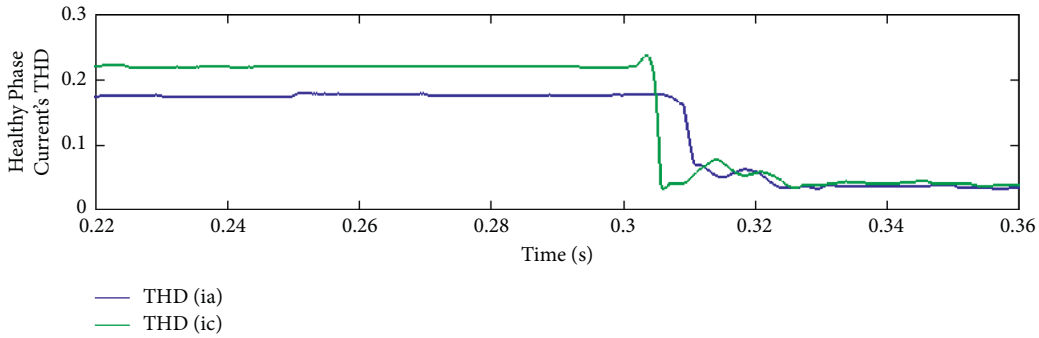

Figure 10: Simulation result of the THD of phases A and C, for open-switch fault and fault-tolerant conditions.

Table 5: Numerical results of the overcurrent indicator and THD for open-switch fault conditions.

Faulty switch	Side phase	Fault condition		Fault-tolerant control	
		I_{ov}	THD	I_{ov}	THD
S_{11}	A	0.62	0.176	0.22	0.035
	C	0.66	0.22	0.21	0.042
S_1 and S_{12}	X	0.44	0.094	0.24	0.034
	C	0.66	0.21	0.35	0.038
S_1 and S_2	X	0.60	0.21	0.35	0.036
	Z	0.62	0.23	0.33	0.037

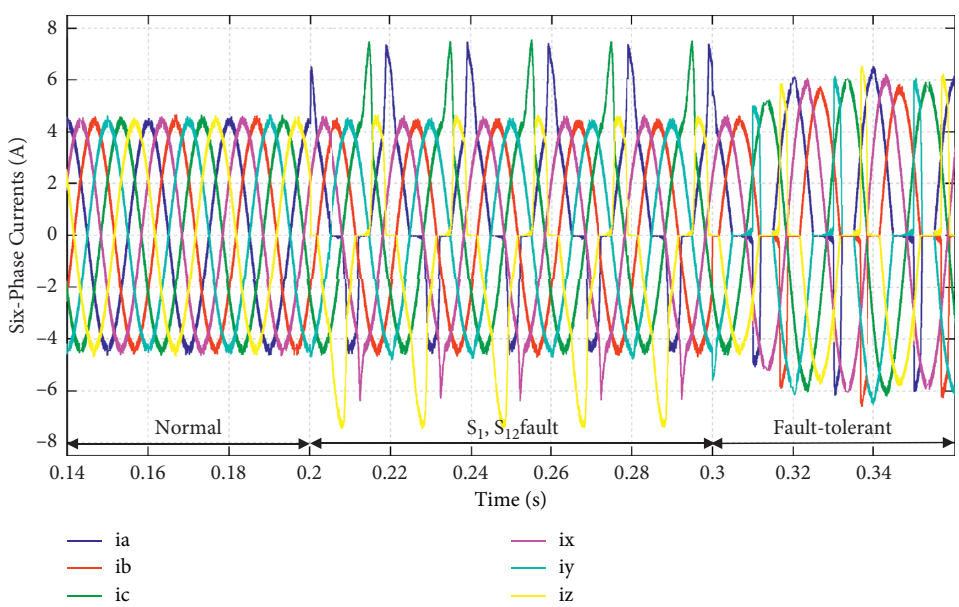

(a)

Figure 11: Continued.

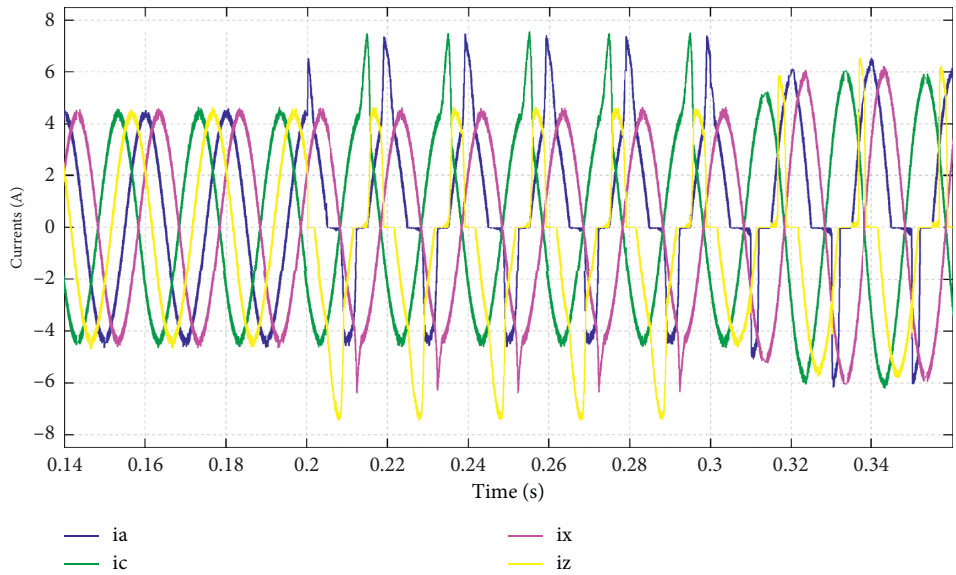

(b)

Figure 11: Simulation result of the AC-DC converter currents before and after multiple open-switch faults in S_1 and S_{12}. (a) All phases. (b) Faulty phases A and Z and side phases X and C.

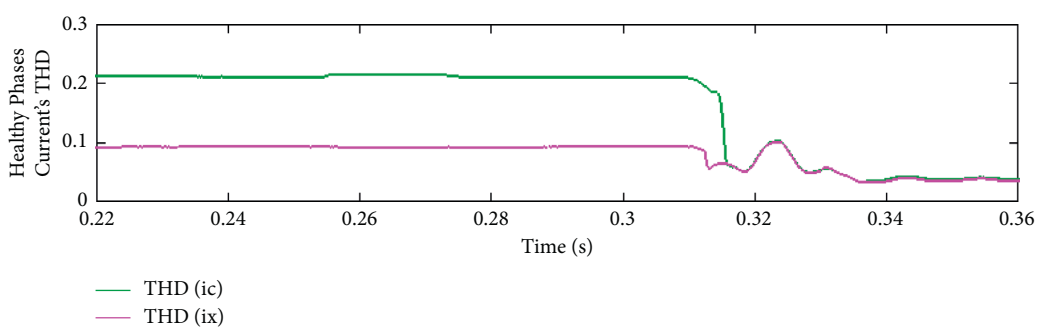

Figure 12: Simulation result of the THD of phases X and C, for multiple open-switch fault and fault-tolerant conditions.

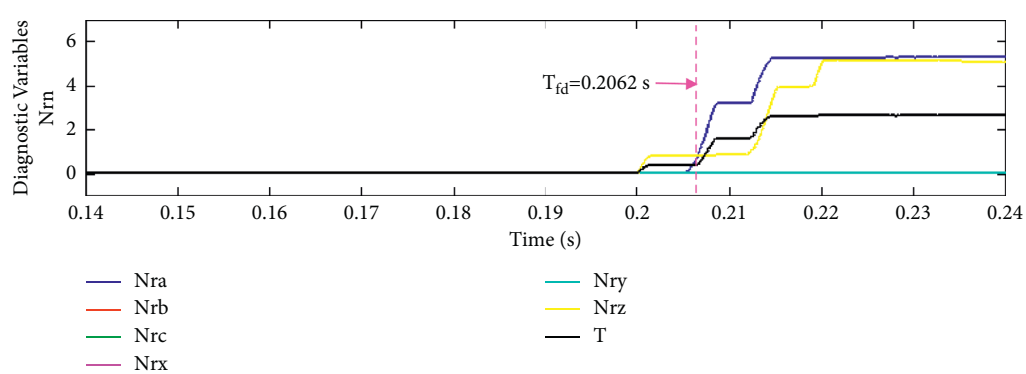

Figure 13: Simulation result of the diagnostic variables Nr_n, for open-switch faults in phases A and Z.

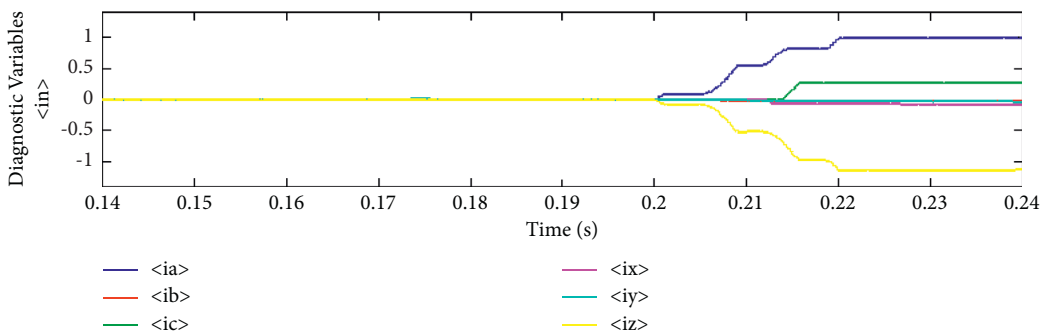

Figure 14: Simulation result of the diagnostic variables $\langle in \rangle$, for open-switch faults in S_1 and S_{12}.

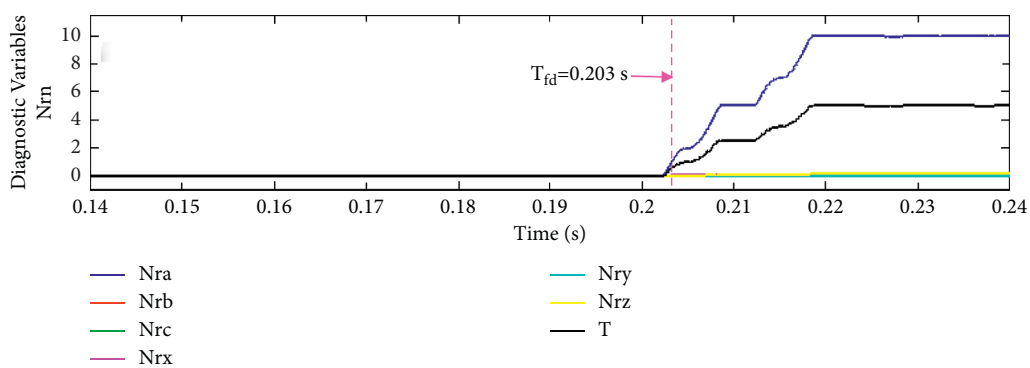

Figure 15: Simulation result of the diagnostic variables Nr_n, for open-switch faults in both switches of phases A.

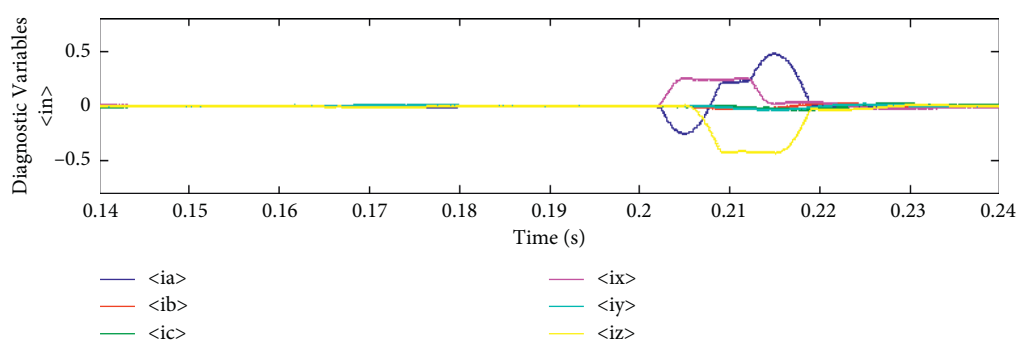

Figure 16: Simulation result of the diagnostic variables $\langle in \rangle$, for multiple open-switch faults in S_1 and S_2.

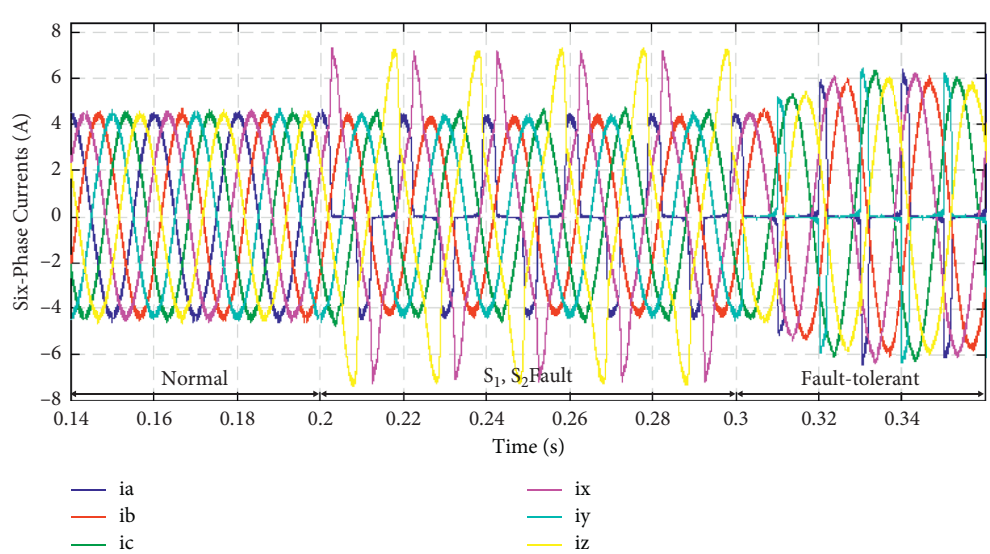

(a)

Figure 17: Continued.

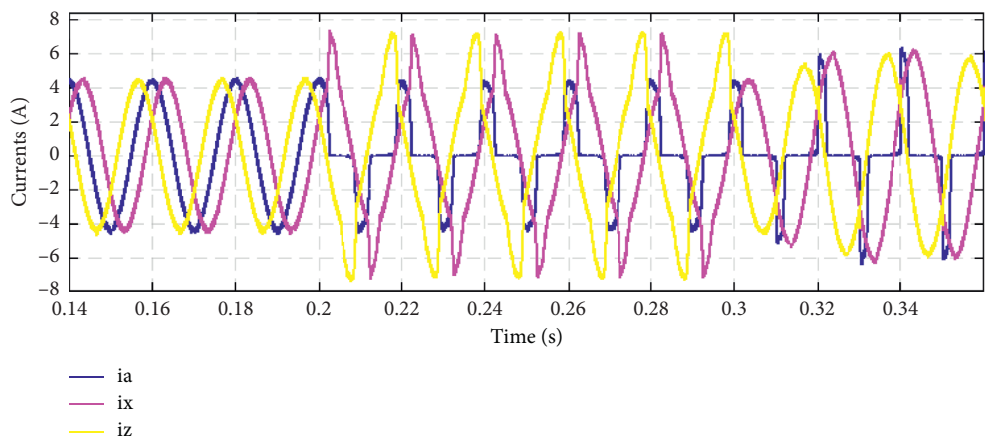

(b)

Figure 17: Simulation result of the AC-DC converter currents before and after multiple open-switch faults in both switches of phase *A*. (a) All phases. (b) Faulty phase A and side phases X and Z.

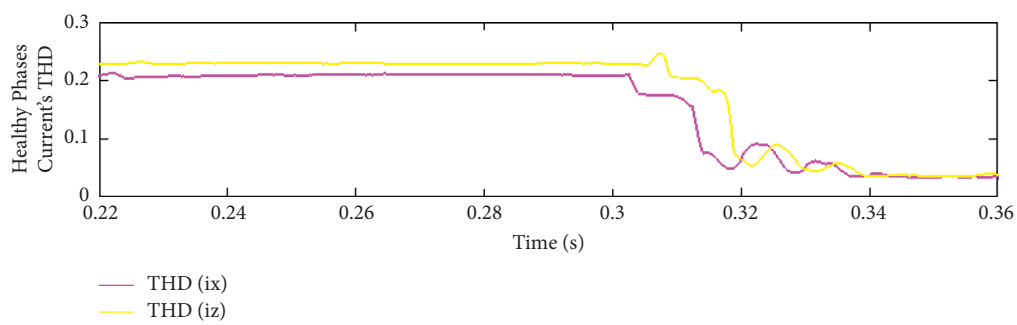

Figure 18: Simulation result of the THD of phases X and Z, for multiple open-switch fault and fault-tolerant conditions.

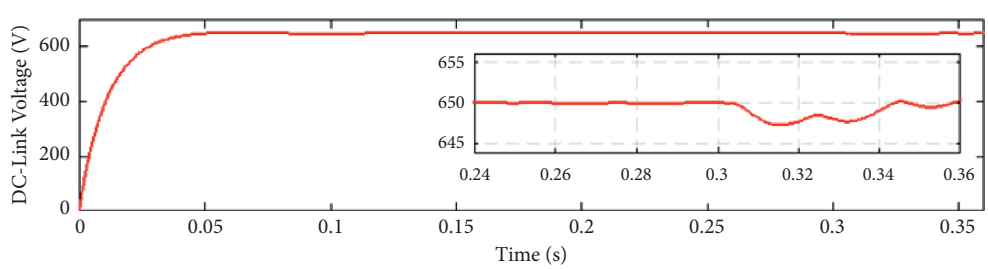

(a)

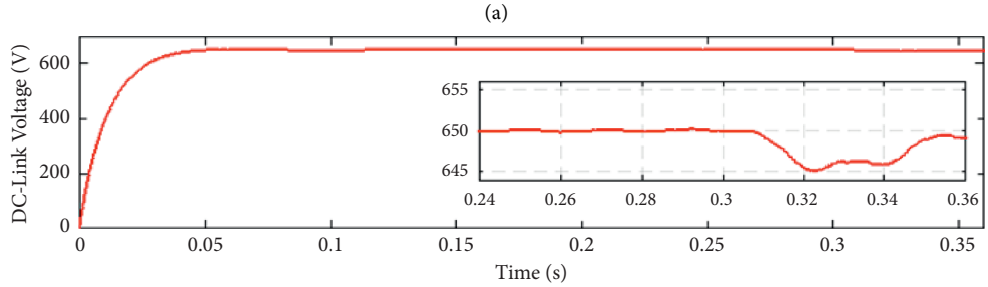

(b)

Figure 19: Continued.

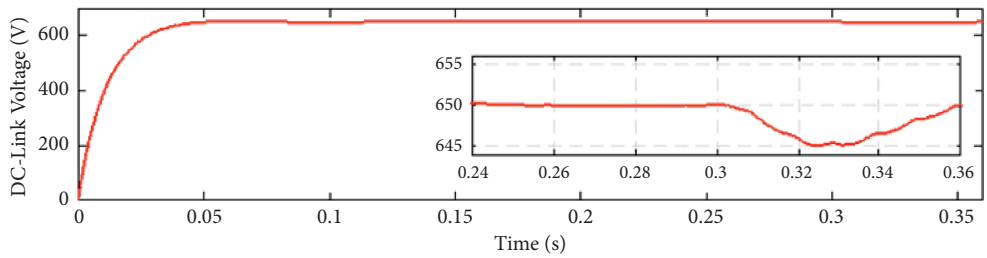

(c)

Figure 19: Simulation result of DC-link voltage ripple, for fault-tolerant conditions. (a) Single open-switch fault. (b) Multiple open-switch faults in different legs. (c) Multiple open-switch faults in one leg.

6. Conclusion

This paper proposes new fault diagnosis and fault-tolerant methods for the six-phase AC-DC converter for single and multiple open-switch faults. The introduced fault diagnosis approach has a simple process, which was integrated with the hysteresis controller, and requires neither complicated calculations, accurate modeling of the system, nor extra hardware. This method is robust against the load changes since a normalized indicator of the fault and an adaptive threshold are used. The main novelty of this research is tolerance against open-switch faults by changing the switching signals in the opposite phase of the faulty phase, without adding any equipment to the circuit. The proposed technique was able to reduce the overcurrent in the side phases, and the value of total harmonic distortion in these phases was also decreased. According to Table 5, in the worst case, at least 20% of the overcurrent value and 6% of the value of total harmonic distortion in side phase (X) were reduced (multiple open-switch faults in S_1 and S_{12}). Moreover, the DC-link voltage is stabilized with an acceptable ripple, which is smaller than 1% of the reference value. The effectiveness of the proposed fault detection and fault-tolerant methods is confirmed by simulation results for a few different single and multiple fault cases. Evaluation of other switching techniques in the open-switch fault condition and implementation of modern controllers can be considered as future topics.

Abbreviations

GSC: Grid side converter
MSC: Machine side converter
PI: Proportional integral
PMSG: Permanent magnet synchronous generator
THD: Total harmonic distortion
TRIACs: Triode for alternating currents.

Symbols

i: Current (A)
L: Inductance (H)
P: Power (w)
R: Resistance (Ω)
T: Adaptive threshold
u: Voltage (V)
w_1: Angular frequency.

Subscripts

d, q: Direct and quadrature components
fd: Fault detection
m: Amplitude value
max: Maximum
min: Minimum
mod: Converter
ov: Overcurrent
ref: Reference
s: Source.

Data Availability

The MATLAB files data used to support the findings of this study are available from the corresponding author upon request.

Conflicts of Interest

The authors declare that they have no conflicts of interest.

References

[1] M. Shahbazi, P. Poure, and S. Saadate, "Real-time power switch fault diagnosis and fault-tolerant operation in a DFIG-based wind energy system," *Renewable Energy*, vol. 116, pp. 209–218, 2018.

[2] M. Nasiri, S. Mobayen, and Q. M. Zhu, "Super-twisting sliding mode control for gearless PMSG-based wind turbine," *Complexity*, vol. 2019, Article ID 6141607, 16 pages, 2019.

[3] C. N. Wang, W. C. Lin, and X. K. Le, "Modelling of a PMSG wind turbine with autonomous control," *Mathematical Problems in Engineering*, vol. 2014, Article ID 856173, 9 pages, 2014.

[4] A. Nahome Alemayehu, R. Zaimeddine, B. Liu, and T. Undeland, "Vector control of direct drive six phase permanent magnet synchronous generators," in *Proceedings of the Conference of IEEE PES PowerTech*, pp. 1–7, Milan, Italy, June 2011.

[5] W. Qiao and D. Lu, "A survey on wind turbine condition monitoring and fault diagnosis-Part I: components and subsystems," *IEEE Transactions on Industrial Electronics*, vol. 62, no. 10, pp. 6536–6545, 2015.

[6] C. Kaidis, B. Uzunoglu, and F. Amoiralis, "Wind turbine reliability estimation for different assemblies and failure severity categories," *IET Renewable Power Generation*, vol. 9, no. 8, pp. 892–899, 2015.

[7] H. Guo, S. Guo, J. Xu, and X. Tian, "Power Switch open-circuit fault diagnosis of six-phase fault tolerant permanent magnet synchronous motor system under normal and fault-tolerant operation conditions using the average current park's vector approach," *IEEE Transactions on Power Electronics*, vol. 36, no. 3, pp. 2641–2660, 2020.

[8] W.-S. Im, J.-M. Kim, D.-C. Lee, and K.-B. Lee, "Diagnosis and fault-tolerant control of three-phase AC-dc PWM converter systems," *IEEE Transactions on Industry Applications*, vol. 49, no. 4, pp. 1539–1547, 2013.

[9] F. Asghar, M. Talha, and S. H. Kim, "Neural network based fault detection and diagnosis system for three-phase inverter in variable speed drive with induction motor," *Journal of Control Science and Engineering*, vol. 2016, Article ID 1286318, 12 pages, 2016.

[10] I. Jlassi and A. J. M. Cardoso, "Fault-tolerant back-to-back converter for direct-drive PMSG wind turbines using direct torque and power control techniques," *IEEE Transactions on Power Electronics*, vol. 34, no. 11, pp. 11215–11227, 2019.

[11] H. Habibi, I. Howard, and S. Simani, "Reliability improvement of wind turbine power generation using model-based fault detection and fault tolerant control: a review," *Renewable Energy*, vol. 135, pp. 877–896, 2019.

[12] I. Jlassi, J. O. Estima, S. K. El Khil, N. M. Bellaaj, and A. J. M. Cardoso, "Multiple open-circuit faults diagnosis in back-to-back converters of PMSG drives for wind turbine systems," *IEEE Transactions on Power Electronics*, vol. 30, no. 5, pp. 2689–2702, 2014.

[13] Y. Mao, T. Peng, H. Han, S. Zhao, and Z. Li, "Open-circuited fault detection on switch of convertor in double-fed wind power generator set based on state observer," *Computer Aided Engineering*, vol. 24, no. 3, pp. 57–61, 2015.

[14] H. Yan, Y. Xu, F. Cai, H. Zhang, W. Zhao, and C. Gerada, "PWM-VSI fault diagnosis for a PMSM drive based on the fuzzy logic approach," *IEEE Transactions on Power Electronics*, vol. 34, no. 1, pp. 759–768, 2018.

[15] S. Karimi, A. Gaillard, P. Poure, and S. Saadate, "FPGA-based real-time power converter failure diagnosis for wind energy conversion systems," *IEEE Transactions on Industrial Electronics*, vol. 55, no. 12, pp. 4299–4308, 2008.

[16] H. Zhao and L. Cheng, "Open-switch fault-diagnostic method for back-to-back converters of a doubly fed wind power generation system," *IEEE Transactions on Power Electronics*, vol. 33, no. 4, pp. 3452–3461, 2017.

[17] A. M. Mendes and A. M. Cardoso, "Voltage source inverter fault diagnosis in variable speed AC drives, by the average current Park's vector approach," in *Proceedings of the IEEE International Electric Machines and Drives Conference*, pp. 704–706, Seattle, Was, USA, May 1999.

[18] A. M. S. Mendes, A. M. Cardoso, and E. S. Saraiva, "Voltage source inverter fault diagnosis in variable speed AC drives, by Park's vector approach," in *Proceedings of the 1998 Seventh International Conference on Power Electronics and Variable Speed Drives*, pp. 538–543, London, UK, September 1998.

[19] N. M. Freire, J. O. Estima, and A. M. Cardoso, "Converters fault-diagnosis in PMSG drives for wind turbine applications," in *Proceedings of the IECON 2010-36th Annual Conference on IEEE Industrial Electronics Society*, pp. 403–408, Glendale, ARI, USA, November 2010.

[20] N. M. Freire, J. O. Estima, and A. J. M. Cardoso, "Open-circuit fault diagnosis in PMSG drives for wind turbine applications," *IEEE Transactions on Industrial Electronics*, vol. 60, no. 9, pp. 3957–3967, 2012.

[21] S. Abramik, W. Sleszynski, J. Nieznanski, and H. Piquet, "A diagnostic method for on-line fault detection and localization in VSI-fed AC drives," in *Proceedings of the 10th European Conference on Power Electronics and Applications*, pp. 1–8, Toulouse, France, September 2003.

[22] S. Khomfoi, W. Sae-Kok, and I. Ngamroo, "An open circuit fault diagnostic technique in IGBTs for AC to DC converters applied in microgrid applications," *Journal of Power Electronics*, vol. 11, no. 6, pp. 801–810, 2011.

[23] J. O. Estima and A. J. Marques Cardoso, "A new approach for real-time multiple open-circuit fault diagnosis in voltage-source inverters," *IEEE Transactions on Industry Applications*, vol. 47, no. 6, pp. 2487–2494, 2011.

[24] I. Jlassi and A. J. M. Cardoso, "IGBTs and current sensors fault diagnosis in direct-drive PSMG wind turbine systems using adaptive thresholds," in *Proceedings of the IECON 2017-43rd Annual Conference of the IEEE Industrial Electronics Society*, pp. 5072–5077, Beijing, China, August 2017.

[25] I. Jlassi, J. O. Estima, S. K. El Khil, N. M. Bellaaj, and A. J. M. Cardoso, "A robust observer-based method for IGBTs and current sensors fault diagnosis in voltage-source inverters of PMSM drives," *IEEE Transactions on Industry Applications*, vol. 53, no. 3, pp. 2894–2905, 2016.

[26] P. Duan, K. G. Xie, L. Zhang, and X. Rong, "Open-switch fault diagnosis and system reconfiguration of doubly fed wind power converter used in a microgrid," *IEEE Transactions on Power Electronics*, vol. 26, no. 3, pp. 816–821, 2010.

[27] A. Mohamed, S. Vanteddu, and O. Mohammed, "Protection of bi-directional AC-DC/DC-AC converter in hybrid AC/DC microgrids," in *Proceedings of the 2012 Proceedings of IEEE Southeastcon*, pp. 1–6, Orlando, FL, USA, March 2012.

[28] M. O. Aboelhassan, T. Raminosoa, A. Goodman, L. De Lillo, and C. Gerada, "Performance evaluation of a vector-control fault-tolerant flux-switching motor drive," *IEEE Transactions on Industrial Electronics*, vol. 60, no. 8, pp. 2997–3006, 2012.

[29] Y. Hu, L. Zhang, W. Huang, and F. Bu, "a fault-tolerant induction generator system based on instantaneous torque control (ITC)," *IEEE Transactions on Energy Conversion*, vol. 25, no. 2, pp. 412–421, 2010.

[30] B. A. Welchko, T. A. Lipo, T. M. Jahns, and S. E. Schulz, "Fault tolerant three-phase AC motor drive topologies: a comparison of features, cost, and limitations," *IEEE Transactions on Power Electronics*, vol. 19, no. 4, pp. 1108–1116, 2004.

[31] R. L. de Araujo Ribeiro, C. B. Jacobina, E. R. C. Da Silva, and A. M. N. Lima, "Fault-tolerant voltage-fed PWM inverter AC motor drive systems," *IEEE Transactions on Industrial Electronics*, vol. 51, no. 2, pp. 439–446, 2004.

[32] N. M. Freire and A. J. M. Cardoso, "A fault-tolerant PMSG drive for wind turbine applications with minimal increase of the hardware requirements," *IEEE Transactions on Industry Applications*, vol. 50, no. 3, pp. 2039–2049, 2013.

[33] N. M. Freire and A. J. M. Cardoso, "Fault-tolerant PMSG drive with reduced DC-link ratings for wind turbine applications," *IEEE Journal of Emerging and Selected Topics in Power Electronics*, vol. 2, no. 1, pp. 26–34, 2013.

[34] W. S. Im, J. J. Moon, J. M. Kim, D. C. Lee, and K. B. Lee, "Fault tolerant control strategy of 3-phase AC-DC PWM converter under multiple open-switch faults conditions," in *Proceedings of the 2012 Twenty-Seventh Annual IEEE Applied Power Electronics Conference and Exposition (APEC)*, pp. 789–795, Orlando, FL, USA, February 2012.

[35] R. Bolbolnia, E. Heydari, and K. Abbaszadeh, "Fault tolerant control in direct-drive PMSG wind turbine systems under open-circuit faults," in *Proceedings of the 2020 11th Power*

Electronics, Drive Systems, and Technologies Conference (PEDSTC), pp. 1–5, Iran, February 2020.

[36] K. Zhou, D. Wang, Y. Yang, and F. Blaabjerg, *Periodic Control of Power Electronic Converters*, Institution of Engineering and Technology, London, UK, 2016.

[37] J. Han, X. Zhou, S. Lu, and P. Zhao, "A three-phase bidirectional grid-connected AC/DC converter for V2G applications," *Journal of Control Science and Engineering*, vol. 2020, Article ID 8844073, 12 pages, 2020.

[38] S. Khojet El Khil, I. Jlassi, A. J. Marques Cardoso, J. O. Estima, and N. Mrabet-Bellaaj, "Diagnosis of open-switch and current sensor faults in PMSM drives through stator current analysis," *IEEE Transactions on Industry Applications*, vol. 55, no. 6, pp. 5925–5937, 2019.

Hindawi
Mathematical Problems in Engineering
Volume 2021, Article ID 3399049, 12 pages
https://doi.org/10.1155/2021/3399049

Research Article

Analyzing Renewable and Nonrenewable Energy Sources for Environmental Quality: Dynamic Investigation in Developing Countries

Itbar Khan,[1] **Lei Han**,[1] **Hayat Khan**,[2] **and Le Thi Kim Oanh**[3]

[1]*Business School of Xiangtan University, Xiangtan, Hunan, China*
[2]*China Center for Special Economic Zone Research, Shenzhen University, Shenzhen, China*
[3]*College of International Education, Guangxi University for Nationalities, Guangxi, Nanning, China*

Correspondence should be addressed to Hayat Khan; khiljihayat@gmail.com

Received 29 June 2021; Revised 16 August 2021; Accepted 30 August 2021; Published 21 September 2021

Academic Editor: Mojtaba Nasiri

Most of developing countries are facing environmental degradation challenges as these countries use energy from fossil fuels to enhance economic activities and that leads to environmental degradation. The use of renewable energy is required to mitigate environmental degradation; however, developing countries may not yet have reached the desired level to acquire renewable energy. It is important for developing countries to make polices to shift from nonrenewable energy to renewable energy use to protect environmental quality. In this regard, the importance of different energy sources and financial development in enhancing environmental quality in 21 developing countries is examined from 1970 to 2018. The study employed dynamic estimator, and the results indicate that the sources of renewable energy enhance environmental quality as compared to nonrenewable energy and its sources. Financial development also lowers environmental quality in our results. The study recommends reducing carbon emissions by reducing the use of fossil fuel energy and acquiring new technologies, attracting foreign investors in clean energy that provide clean technologies for green production, and investing in renewable energy sources to evade nonrenewable energy. Policy makers should adopt environmentally-friendly strategies and equipment to protect environmental quality, while striving for achieving economic growth.

1. Introduction

Developing countries are trying to raise the level of economic growth and development by establishing policies which are helpful to increase the investment level. An economy can grow if it is enough developed financially. Financial institutions are important for a country to enhance investment by providing credit facilities and provide opportunities of capital. Financial development promotes the energy sector which accelerates economic activities [1]. Energy consumption also plays an important role to enhance economic growth by facilitating production with capital and labor. Both financial development and energy consumption promote production levels and economic growth, but they increase carbon emissions and cause environmental degradation [2]. The use of energy is important to promote economic activity, and it also creates environmental-related problems, such as the depletion of natural resources and carbon emissions. In this context, developing countries urgently need to promote economic growth. Therefore, for decades, they have widely used fossil fuel energy to promote economic and developmental activities. The reason of environmental degradation faced by developing countries is the reason of energy from fossil fuels being used to increase economic activities. Increasing these activities for the purpose to enhance economic growth in developing countries is important; however, the quality of environment also needs to be protected. In such cases, fossil fuels are used in industries to enhance economic growth, which leads to degrading of the environment as industries have high demand for energy and thus use fossil fuels to meets their increasing demand. Wolde-Rufael and Menyah [3] argue

that environmental degradation is the reason of nonrenewable energy use as it releases high amount of carbon dioxide. The use of renewable energy sources that includes wind, hydro, and solar can be the substitute to overcome such environmental issues. The use of renewable energy can fulfil the production requirement for energy and enhance environmental quality as well as it does not cause pollution by replacing nonrenewable technologies and does not degrade environmental quality [4, 5]. On the contrary, some studies suspect the role of renewable energy in environment protection such as Jebli and Yossef [6] claim that waste and combustible renewables are not clean energy and the use of combustible renewables and wastes increases emission. However, the theoretical literature considers that renewable energy consumption is beneficial for environment quality; however, some studies have given mixed results. Some studies indicate that renewable energy usage reduces carbon emission such as [5, 7–13], while some studies argue that renewable energy usage increases emission such as [14–16]. On the other side, some of the previous studies claim that there is no effect or insignificant impact of renewable energy on carbon emission [17]. Developing countries should especially focus to make polices and convert from nonrenewable sources of energy and invest in projects to convert to renewable energy. Financial sector contribution is also important to fund green energy projects to facilitate renewable energy. The developing countries' financial development can enhance the renewable energy if it is well developed. The improvement in financial sectors and energy in turn keeps enhancing the level of economic growth as well can achieve higher environmental quality in developing countries. Based on the ongoing debate on the role of renewable and nonrenewable energy sources usage in carbon emission and considering environmental degradation as a global challenge for countries, especially for developing countries, requires empirical research and policy implications. The current study, therefore, examines both renewable and nonrenewable energy and its sources on carbon emission to identify the contribution of each energy sources to environmental quality. The focus of the study is to determine that whether conversion from nonrenewable energy to renewable energy may significantly improve the environmental quality of the sample countries. In our research, we also pay attention to the impact of financial development on carbon emissions. The developed financial system can promote renewable energy projects. Green finance can help improve the quality of the environment. However, if financial development does not fund renewable energy projects, finance will cause environmental degradation. The study used the latest data downloaded from BP statistics and World Development Indicators between 1970 and 2018. This study implemented static and dynamic models including OLS, FE, and SGMM and examined the impact of energy use on carbon emissions in developing countries. Based on the above discussion, this research is very important for developing countries to obtain advice when using nonrenewable energy to promote their economic growth. The study was implemented for the first time and provided very useful suggestions for the sample countries to invest in renewable energy projects to meet the energy needs of production and achieve higher environmental quality. It is better to invest in the energy sector than to focus solely on economic growth because in the long run, investing in renewable energy projects can bring double benefits, economic growth and environmental quality. Our results confirm that the use of nonrenewable energy sources for production in developing countries leads to degradation of the environment, while renewable energy sources are the safeguard of environmental quality. Financial development in the sample countries has also been found a weak determinant to enhance environmental quality which needs attention. The countries should strengthen financial institutions to fund renewable energy projects.

The rest of the paper is structured in the given sequence. Section 2 is composed of related literature, Section 3 presents the study methodology, Section 4 is composed of empirical results and discussion, while Section 5 gives the conclusion and policy implication.

2. Literature Review

A large number of existing studies uses panel and time series data and conduct research studies on the impact of the use of renewable and nonrenewable energy on environmental quality in samples of different countries and regions and have achieved different results. For example, Zaidi et al. [18] examined carbon emission and renewable and nonrenewable energy in Pakistan. They used ARDL estimator and found insignificant effect of renewable energy while positive effect of nonrenewable energy on carbon emission. In case of sub-Saharan Africa, Hanif [19] investigated the same association and found that the influence of renewable energy is smaller on carbon emission. Similarly, in [20], the authors studied energy use and carbon emissions from 1980 to 2015 and found that the impact of natural gas and oil on carbon emissions is asymmetric. They further discovered that the impact of nonrenewable energy on carbon emissions varies from country to country. Khan et al. [21] studied the impact of energy consumption on carbon emissions from 1965 to 2015 and found that there is a short-term and long-term relationship between variables and carbon emissions. They believe that renewable energy usage reduces carbon emissions. In the United States, Ongan et al. [22] studied the impact of renewable energy and fossil fuels on carbon emissions. They proved the EKC hypothesis in their findings and pointed out that fossil fuels have a negative impact on Texas' carbon emissions, while energy consumption increases Florida's emissions. Anser et al. [23] studied renewable and fossil fuels energy along industrial growth on carbon emission in Caribbean and Latin America for the year 1990 to 2015. They used the two-step system GMM model and found the inverted U-shaped relationship of carbon emission and economic growth which is evident in EKC hypothesis. They further found that industrial growth and fossil fuels' energy increase carbon emission. Zhao et al. [24] investigated the effect of energy consumption and geopolitical risk on carbon

emission in BRICS countries. They used the ARDL method and found that geopolitical risk negatively affects energy consumption in some countries as well carbon emission in few countries. They further state that a decrease in geopolitical risk negatively and positively affects carbon emission in different countries of BRICS. Karimi et al. [25] studied the association of renewable energy, economic growth, and carbon emission in Iran for the period of 1975 to 2017. They used cointegration and asymmetric method where the findings indicate that renewable energy use and carbon emission increase economic growth in the long run, while decrease in renewable energy also has the same effect; however, economic growth strongly increases renewable energy. They further found that carbon emission has insignificant impact on economic growth. Yuping et al. [26] studied the effect of renewable and nonrenewable energy use and globalization on carbon emission in Argentina from 1970 to 2018. They used the ARDL model and found that globalization and renewable energy consumption reduce, while nonrenewable energy increases emission in short as well in the long run. On the contrary, Majeed and Luni [27] used panel data from 166 countries to study the impact of water withdrawal, energy use, and economic growth on carbon emissions. Their research period was 1990–2017, and they used two-stage least squares and fixed and random effects' models. They found that the use of renewable energy had a negative impact on emissions and that water intake would increase emissions. They further proved the EKC hypothesis. Khan et al. [28] studied the impact of foreign direct investment on carbon emissions in developing and developing countries. Using long-term estimates and static and dynamic models, they found that the impact of trade openness on carbon emissions in developing countries is diminishing, while the impact of trade on carbon emissions in developing countries is the opposite. They further formulated regulations for renewable energy to reduce emissions in developed and developing countries. Likewise, in [29], the authors believe that it is difficult for developing countries to switch from fossil fuels to renewable energy, and because the economic and technological level and energy structure are different in developing and developed countries, the transition from developing countries to renewable energy is a challenge. Similarly, Khan et al. [28] studied trade, foreign direct investment, and carbon emissions in developing countries. Using static, dynamic, and long-term estimates, they found that open trade and renewable energy use reduced carbon emissions in developing countries. They also pointed out that foreign direct investment has increased emissions in developed countries, while reducing emissions in developing countries. Similarly, in [29], the authors believe that it is a challenge for developing countries to switch from fossil fuel energy to renewable energy use. Due to different economic and technological conditions, the energy structure of developing countries and developed countries is different, which is why it is difficult for developing countries to switch to renewable energy. Ali et al. [30] investigated the impact of Pakistan's energy consumption, financial development, and trade on carbon emissions from 1980 to 2015. Applying ADF testing and ARDL to the data, it is found that the influence of research variables is increasing with regard to carbon emissions. For a summary of the relevant literature on the impact of renewable energy and nonrenewable energy consumption on carbon emissions, detailed information is given in Table 1 below.

On the contrary, Khan et al. [43] examined energy consumption, the inflow of foreign direct investment, and carbon emissions in the global countries. They found the interinfluence of these variables on each other, while the consumption of renewable energy has reduced carbon emissions and, at the same time, reduced the inflow of FDI. They found that FDI promotes economic growth, while the use of renewable energy reduces economic growth. However, as Khan et al. [44] pointed out by studying the impact of FDI inflows in Pakistan on governance, the increase in FDI is the cause of good governance. They found that governance indicators are important to the increase in FDI inflows. Cetin et al. [45] examined trade openness, economic growth, and energy consumption in Turkey. Their study time period was from 1960 to 2013, and they found that trade, energy consumption, and financial development have long-run association.

Likewise, Dogan and Ozturk [8] investigated carbon emission and nonrenewable and renewable energy in US for the time 1980 to 2014. They found the existence of cointegration of the study variables, while the ARDL results show that carbon emission is reduced by the use of renewable energy, while increased by nonrenewable energy use. However, they found that the EKC assumption is invalid for the United States of America. Khan et al. [46] studied trade, quality institutions, and innovation of global carbon emissions. They found that open trade and FDI reduced carbon emissions, where the impact of institutional quality indicators was significant for carbon emissions. They further found the increasing influence of innovation in emission. Similarly, Bhat [47] studied the carbon emissions of renewable and nonrenewable energy in a sample of five emerging countries from 1992 to 2016. They employed the panel model and found that capital and labor were positively correlated in long run with nonrenewable energy; however, the impact of renewable energy on carbon emissions was insignificant. Similarly, Khan et al. [48] studied the relationship between environmental factors in the global panel by considering the technological progress and institutional quality in the association. They used static and dynamic GMM to discover the positive impact of technology progress, financial development, and the use of nonrenewable energy on carbon emissions, while the negative impact of renewable energy and FDI on carbon emissions. However, in their research results, the impact of institutions on carbon emissions is negative. Ito [9] studied carbon emissions, renewable energy consumption, nonrenewable energy consumption, and economic growth and found that the consumption of nonrenewable energy has a negative impact on economic growth, while the consumption of renewable energy has a positive impact on the economic growth of developing countries.

Table 1: Summary of literature.

Study	Time	Main variables	Countries	Methodology
Alqaralleh [31]	2000–2018	CO2, GDPPC, RE, NRE, and POP	30 European countries	Panel smooth transition regression
Fatima et al. [32]	1998–2014	GDPPC (per capita GDP), RE, NRE, TO, and CO2	High emitter countries	Kao cointegration, GMM, and random and fixed effect
Ibrahim and Ajide [33]	1990–2018	Coal, gas, fuel, TO, and CO2	G-20 countries	Augmented mean group (AMG), common correlated effect mean group (CCEMG), and mean group
Sharma et al. [34]	1990–2016	Stock market, GDPPC, TO, RE, and technological innovation	South Asian countries	CS-ARDL
Fu et al. [35]	-	RE, CO2, and economic growth	BRICS countries	"Cross-dependency" test, the unit root test, and "CIPS" IPS, DOLS, and FMOLS
Kula [36]	1980–2008	GDP and RE	OECD countries	Pedroni cointegration tests, DOLS, and VECM Granger causality test
Charfeddine and Kahia [37]	1980–2015	GDP, CO2, REC, LF, and FD	Middle East and North Africa, 24 countries	Panel VAR model and Westerlund ECM panel cointegration test
Adewuyi and Awodumi [38]	1980–2010	GDP, CO2, RE, FD, POP, and TO	West African countries	Three-stage least squares (3SLS)
Inglesi-Lotz [39]	1990–2010	GDP, RE, and LF	OECD countries	FE and panel cointegration test REC
Cho et al. [40]	1990–2010	GDP, RE, and LF	31 OECD and 49 non-OECD countries	Panel VECM and FMOLS
Dogan [41]	1990–2012	GDP, REC, NRE, and LF	Turkey	ARDL bounds test, Johansen panel cointegration, and Gregory–Hansen cointegration tests
Shahbaz et al. [42]	1972Q1–2011Q4	REC, LF, and capital formation	Pakistan	ARDL bounds test and VECM Granger causality test

Source: author tabulation.

3. Methodology

3.1. Empirical Models and Variables. This study investigates the role of renewable and nonrenewable energy use in environmental quality for the period of 1970 to 2018 in 21 developing countries listed in Table 2. The nonrenewable energy sources used in this study are coal, oil, and natural gas, while the renewable energy sources used in this study are wind, solar, and hydropower, which are collected from BP statistics. Similarly, the study also used fossil fuel energy consumption collected from WDI (World Development Indicators) as a percentage of total final energy consumption and renewable energy consumption (percentage of total final energy consumption). Financial development is also used, expressed as a percentage of GDP in private sector domestic credit. The control variables used in the study are urban population and labor force.

The list of variables and data sources is shown in Table 3, and the conceptual model is shown in Figure 1. First, this study examines the impact of renewable energy sources and financial development on carbon emissions. Second, the study examines the impact of nonrenewable energy sources on carbon emissions. Next, we study the effects of the total renewable energy consumption and nonrenewable energy consumption in equations (3) and (4), respectively. The following models have been built:

Table 2: List of countries.

Bangladesh	Iran Islamic Rep	Singapore
Brazil	Iraq	South Africa
Chile	Israel	Sri Lanka
China	Pakistan	Turkey
Colombia	Philippines	United Arab Emirates
Ecuador	Qatar	Venezuela
Egypt Arab Rep.	Saudi Arabia	RB Vietnam

$$\begin{aligned} CO_2 = {} & \beta_0 + \beta_1 SLR_{it} + \beta_2 HDR_{it} + \beta_3 WND_{it} \\ & + \beta_4 FD + \beta_5 UOP + \beta_6 LF + \varepsilon_{it}, \end{aligned} \tag{1}$$

$$\begin{aligned} CO_2 = {} & \beta_0 + \beta_1 OL_{it} + \beta_2 GS_{it} + \beta_3 CL_{it} \\ & + \beta_4 FD + \beta_5 UOP + \beta_6 LF + \varepsilon_{it}, \end{aligned} \tag{2}$$

$$CO_2 = \beta_0 + \beta_1 RET_{it} + \beta_2 FD_{it} + \beta_3 UOP_{it} + \beta_4 LF + \varepsilon_{it}, \tag{3}$$

$$CO_2 = \beta_0 + \beta_1 ENT_{it} + \beta_2 FD_{it} + \beta_3 UOP_{it} + \beta_4 LF + \varepsilon_{it}. \tag{4}$$

In above equations, carbon dioxide is represented by CO_2 used for environmental degradation, SLR is solar energy, HDR is hydropower, WND is wind energy, FD is the financial development proxy by private sector domestic credit, RET is the total renewable energy consumption, ENT

Table 3: Variables and data sources.

Variables	Symbols		Data source
Carbon emission	CO2	—	WDI
Oil	OL	Nonrenewable energy sources	BP statistics
Coal	CL		BP statistics
Natural gas	NG		BP statistics
Hydroelectricity	HDR	Renewable energy sources	BP statistic
Solar energy	SLR		BP statistics
Wind energy	WND		BP statistics
Renewable energy consumption	RET	—	WDI
Nonrenewable energy consumption	NRT	—	WDI
Financial development	FD	—	WDI
Urban population	UP	—	WDI
Labor force	LF	—	WDI

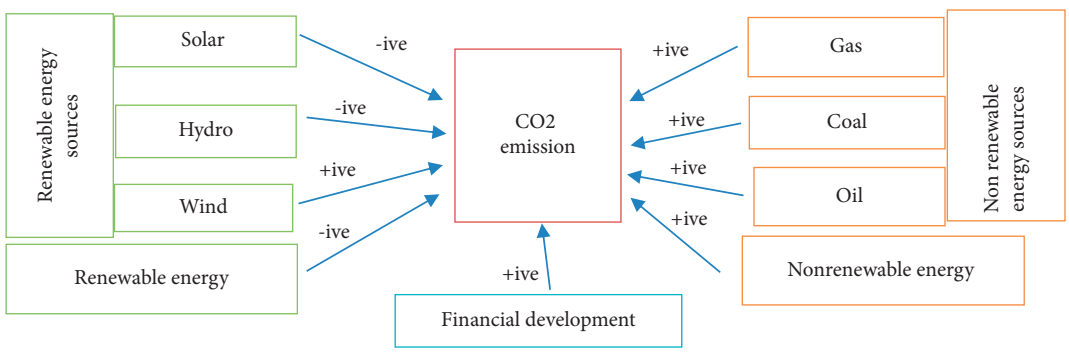

Figure 1: The impact of renewable and nonrenewable energy on carbon emission.

is nonrenewable energy, UOP is the urban population, LF is the labor force, and ε is the error term.

3.2. Econometric Models. The current study explores the impact of energy sources and financial development on carbon emission. Three econometrics techniques were employed to the data which are OLS, fixed effect, and system GMM [49]. System GMM is the recent application concerning the theme; therefore, the current study is focusing on the object, and results are mostly concerned on this. In the first phase, the study has made the OLS and FE method estimation which is used for inspecting the issues of heterogeneity of countries. The GMM techniques are in the first difference and its permit taking to deal with the endogeneity problem concerned with variables of the study. System GMM has the ability to deal with the grouping of both difference and equations in the level. The instruments which specified for the difference equations are variables' delayed values in levels. Furthermore, the variables of the study are instrumented by the level equation and first differences. The system of the equations has been estimated by generalized method of moments simultaneously. The simulation about this of Monte Carlo made by Blundell and Bond [50] stated that SGMM model is efficient the most to estimate such issues. The overidentifying restriction tests are the Sargan test replaced as the Hansen test, and also, the serial correlation test of Arellano and Bond is used. Most of the results regarding these tests confirmed our study expectations. The Hansen test value gives the acceptance and shows the validity of the instruments. The serial correction tests shows whether the hypothesis is validated of second serial correlation of residuals. In the results of regression, the SD of coefficients is validated and heteroscedasticity problem has been checked. OLS and FE static models are employed along the SGMM model because to compare the results and check the robustness with preceding studies' outcomes; however, we especially focus on the system GMM results. The reason is that static models' results may not be efficient as these models may have several econometric issues, and the GMM model is considered the most efficient estimator. The equation for the system GMM model is given below:

$$CO_{2it} = \beta_0 + \beta_1 CO_{2i,t-1} + \beta_2 Y_{i,t} + \beta_3 X_{i,t} + \varepsilon_{i,t}, \quad (5)$$

where CO_2 is carbon emission, Y is the explanatory variable used in the study, X represents the control variables, and $CO_{2i,t-1}$ is the lag of the dependent variable, while ε is the error term.

4. Findings and Discussions

4.1. Renewable Energy Sources and Environmental Degradation. The lagged dependent variable is significant as given in Table 4, which validates the model fitness. AR2 and Sargan test also validate the instruments used in the model.

The impact of hydro energy on carbon emissions is significant at the level of 1% in the three measurements, and the impact on carbon emissions is negative. This shows that, in the sample of 21 developing countries, the increase in

Table 4: The impact of renewable energy sources on carbon emission.

Dependent variable: CO_2	OLS regression	Fixed effect	System GMM
HDR (hydro energy)	−1.970*** (0.247)	−0.024*** (0.006)	−0.007*** (0.001)
SLR (solar energy)	−0.556*** (0.106)	−0.256** (0.109)	−0.181*** (0.013)
WND (wind energy)	0.337* (0.191)	0.072 (0.057)	0.031*** (0.002)
FD (financial development)	0.020*** (0.006)	0.003 (0.005)	0.001** (0.0005)
UP (urban population)	3.130*** (3.920)	3.870 (2.730)	5.100*** (9.861)
LF (labor force)	−1.350*** (2.320)	−3.130** (1.512)	−2.880*** (7.221)
$CO_{2i,t-1}$	—	—	1.005*** (0.087)
Constant	2.909***	60.48**	0.000 (0.000)
Obs	43	59	506
Number of id	—	5	21
R-squared	0.937	0.937	—
AR1	—	—	−2.64 (0.008)
AR2	—	—	−1.67 (0.094)
Sargan test	—	—	859.20 (0.000)

Note: ***, **, and * show the significance level at 1, 5, and 10 percent, respectively. Data source: BP statistics and WDI.

water energy reduces carbon emissions. More specifically, the results of the system GMM show that if hydropower is increased by 1 percentage point, carbon emissions will be reduced by 0.007 percentage points. The results confirmed that hydropower energy is beneficial to environmental quality, supports the theory of social choice, and confirms the theory of environmental degradation that human activities lead to environmental degradation. Countries still need to use the domestic new energy technology market to explore the field of renewable energy, but under current economic conditions, developing countries may not be able to obtain financial support for new technologies. It can be suggested that developing countries should promote and attract foreign investors who use green technologies in production. Similarly, solar energy is also very important as a source of renewable energy. The negative coefficient shows that it reduces carbon emissions and improves environmental quality. The results further show that if there is a unit change in solar energy, the carbon emissions will be reduced by 0.55, 0.25, and 0.18%, respectively, indicated by OLS, FE, and system GMM. Solar energy is conducive to environmental quality and overcoming the energy crisis, especially in developing countries. Nowadays, some developing countries are facing energy crisis. They are trying to introduce solar energy for consumption, but they also need funds to obtain such technologies. Therefore, countries should also focus on economic development to overcome the energy crisis and protect the environment.

The estimated coefficient of wind energy on carbon emissions is significant, and its impact of carbon emissions is positive. The results show that due to the limited technology market in developing countries, the renewable energy sector, such as wind energy, may not be well developed. Alternative energy sources such as natural gas have also reduced attention to the development of the renewable energy sector because natural gas is easily used as an energy source, but natural gas consumption is harmful to the environment. Another reason may be that low-income countries may not be able to explore and fund renewable energy. The financial crisis has also reduced the level of investment and affected the exploration and development of the renewable energy sector. Technical standards lack of the reduction rate of renewable energy investment costs.

The estimated coefficient of domestic credit to the private sector (financial development) is highly significant and positive in OLS and system GMM, but not significant in the fixed effects' model. The results show that financial development has increased the carbon emissions of developing countries. The system GMM results show that a unit excess of domestic private sector credit will increase carbon emissions by 0.001%. This is also determined by [51–56]. These differences may be due to different countries and different sample sizes.

Similarly, the urban population coefficient is significant and positive in the OLS regression and the system GMM model, indicating that the increase in urban population significantly increases carbon emissions. Urbanization is an important factor in increasing carbon emissions because as the population increases, the demand for transportation and energy increases, which in turn increases carbon emissions. Our results are consistent with the findings of Poumanyvong and Kaneko [57] but contrary to those of Rauf et al. [58]. Due to size and sample, results may vary. The labor force in the model shows that it reduces carbon emissions. The system GMM results show that, in the sample countries of developing countries, the percentage change in the labor force can reduce carbon emissions by 2.88%.

4.2. Nonrenewable Energy Sources and Environmental Quality. Developing countries still rely mainly on nonrenewable energy use for production, such as coal, oil, and natural gas, which leads to environmental degradation. The results of the impact of nonrenewable energy on carbon emissions are shown in Table 5. Table 5 below shows the results of the Sargan test and AR2 correlation test, which support the effectiveness of the current research model tools. The estimated coefficient of coal as a nonrenewable energy source is positive and significant in all three models. The results showed that the use of coal energy increased the carbon emissions of the sample countries. More specifically, the system GMM results show that if there is a unit change in

coal energy consumption, carbon emissions will increase by 0.005%. The research results further show that coal energy is a nonrenewable energy source and is harmful to environmental quality. The result was supported by [42, 59, 60].

The survey results further guide countries' policies to reduce carbon emissions by reducing the use of coal energy because coal will increase carbon dioxide emissions and enhance technologies that may help reduce environmental impact. Since our research sample is developing country rather than a developed country, it is still possible to use coal as an energy source, which is more harmful to the environment, but compared to using coal, using natural gas may be better because natural gas consumption may not be as bad as coal. The economic growth of these countries may not be conducive to the financing of renewable energy projects to obtain renewable energy, so it can be suggested that natural gas may be better than coal consumption, but in the future, these countries should strive to promote economic growth and invest in renewable energy to avoid the use nonrenewable energy sources such as coal and natural gas. Alkhathlan and Javid [61] also pointed out that compared with other nonrenewable energy sources, Saudi Arabia uses natural gas better, but the effect of coal on carbon emissions is the opposite. Similarly, the results of the natural gas coefficients in the three models are also significant, and the impact on carbon emissions is positive, indicating that the use of natural gas energy has an increasing impact on carbon emissions, leading to environmental degradation. The results of the system GMM model show that, for every 1% increase in natural gas energy use, the carbon emissions of the sample countries will increase by 0.001%. However, it is believed that natural gas is much lower than other fossil fuels such as coal or oil.

Similarly, oil consumption as a nonrenewable energy source has a positive and significant impact on carbon emissions in all estimators. The results show that petroleum energy has increased the carbon emissions of the sample countries. From these results, it can be seen that oil is still used as the energy source in developing countries, which will indeed reduce the quality of the environment. Our results are consistent with the results of [52, 62, 63].

In all estimates, financial development has a positive impact on carbon emissions. The research results show that financial development is the reason for the increase in carbon emissions in developing countries. The system GMM results show that, for every additional unit of credit in the private sector, carbon emissions will increase by 0.001%, while the urban population coefficient is negatively correlated with carbon dioxide emissions. The labor force is positive and significant in OLS and FE, but the result is not significant and negative in the system GMM model, indicating that when labor is used as a control variable for the impact of nonrenewable energy on emissions, labor has no effect on carbon emissions.

4.3. Total Renewable Energy Consumption and Carbon Emission. Table 6 shows the results of the impact of renewable energy consumption on carbon emissions, where the RET estimation coefficient is negative and significantly confirms that it reduces carbon emissions. For example, a unit change of RET reduces carbon emissions by 0.38, 0.31, and 0.18, respectively, shown by OLS, FE, and SGMM. Our research results support modern ecological theory, emphasizing that the increase in technology and innovation will improve environmental quality. Bilgili et al. [5] also pointed out that the use of renewable energy can improve environmental quality because it replaces traditional machinery and technologies that rely on fossil fuels. Compared with the use of traditional energy, the use of renewable energy will not cause a burden on the environment and sustainability and can also ensure energy security. Our research results are consistent with the results of Sharif et al. [13].They also proved that the impact of renewable energy consumption on carbon emissions is decreasing. Our research results are consistent with the claimed impact of renewable energy on carbon emissions [13, 64].

Similarly, the urban population coefficient is highly significant and positive in both the OLS regression and the system GMM model, indicating that the increase in urban population significantly increases carbon emissions, while it is negatively significant in the fixed effects model. The estimated coefficient of financial development is significant and positive in all models. The results show that financial development has increased carbon emissions in developing countries. System GMM results show that if domestic credit to the private sector increases by 1%, it will increase carbon emissions by 0.183%. The labor force in the OLS and system GMM models shows that it reduces carbon emissions. The system GMM results show that the percentage change in the labor force in developing countries reduces carbon emissions by 0.35%, while the result in the fixed effects model is negative and significant.

4.4. Total Nonrenewable Energy Consumption and Environmental Degradation. Several researchers have debated that those developing countries are trying to increase economic growth and that is why these developing countries depend on nonrenewable energy to increase economic activities as these countries have not yet reached the level to fully use renewable energy for production in order to increase economic growth. The use of nonrenewable energy in these countries may lead to degradation of environment. For this purpose, to identify whether there exists the positive impact of nonrenewable energy used by these countries, we investigate this association, and the results are shown in Table 7. The results indicates that the use of nonrenewable energy reduces the quality of environment by increasing carbon emission. For instance, the GMM results show that a percent increase in NRT causes an increase in emission by 1.26 percent. The results are in line with Table 4 findings, and they are also reinforced by the outcomes of Danish and Wang [65]. Previous studies have also shown that nonrenewable energy sources will reduce environmental quality by increasing carbon emissions. Most of the nonrenewable resources are used to promote economic growth in developing countries, which is the reason for the deterioration of the environment in these developing countries. The

Table 5: The effect of nonrenewable energy sources on carbon emission.

Dependent variable: CO_2	OLS regression	Fixed effect	System GMM
CL (coal)	0.001** (0.000)	0.001*** (0.000)	0.005* (0.002)
NG (natural gas)	0.007** (0.003)	0.004*** (0.000)	0.001** (0.000)
OL (oil)	0.021*** (0.002)	−0.002** (0.001)	0.031*** (0.011)
FD (financial development)	0.011***(0.001)	0.005*** (0.000)	0.001** (0.000)
UP (urban population)	−2.380*** (2.500)	−6.430** (2.570)	−0.025* (0.015)
LF (labor force)	4.550*** (1.220)	1.780***(3.220)	−0.006 (0.013)
Constant	0.527*** (0.103)	0.235** (0.093)	0.496*** (0.187)
$CO_{2i,t-1}$	—	—	0.954* (0.011)
Obs	506	506	413
No. id	21	21	18
R^2	0.378	0.413	—
AR1	—	—	−8.28 (0.000)
AR2	—	—	−1.60 (0.109)
Sargan test	—	—	387.15 (0.730)

Note: ***, **, and * show the significance level at 1, 5, and 10 percent, respectively. Data source: BP statistics and WDI.

Table 6: The effect of renewable energy consumption on carbon emission.

Dependent variable: CO_2	OLS regression	Fixed effect	System GMM
RET (renewable energy consumption)	−0.387*** (0.013)	−0.312*** (0.039)	−0.183*** (0.046)
FD (financial development)	0.013*** (0.000)	0.005*** (0.000)	0.200*** (0.022)
UOP (urban population)	3.530*** (9.341)	−7.971** (6.821)	1.910** (7.111)
LF (labor force)	−2.780*** (6.731)	8.720*** (1.950)	−0.357* (0.189)
Constant	1.185*** (0.059)	0.964*** (0.130)	0.000*** (0.000)
$CO_{2i,t-1}$	—	—	0.889*** (0.030)
Obs	479	479	479
R^2	0.712	0.481	—
No. id	—	20	20
AR1	—	—	−1.45 (0.147)
AR2	—	—	−0.92 (0.357)
Sargan test	—	—	426.46 (0.950)

Note: ***, **, and * show the significance level at 1, 5, and 10 percent, respectively. Data source: BP statistics and WDI.

Table 7: Total nonrenewable energy consumption on carbon emission.

Dependent variable: CO_2	OLS regression	Fixed effect	System GMM
NRT (nonrenewable energy use)	0.053*** (0.001)	0.034*** (0.001)	1.269** (0.607)
FD (financial development)	0.007*** (0.001)	0.002*** (0.000)	0.085*** (0.025)
UP (urban population)	2.490** (9.771)	1.630*** (5.721)	3.720*** (2.750)
LF (labor force)	−2.460*** (7.031)	7.791 (1.690)	−0.961*** (0.301)
Constant	−3.456*** (0.134)	−1.831*** (0.135)	0.000*** (0.000)
$CO_{2i,t-1}$	—	—	1.028 (0.031)
Observations	493	493	493
R^2	0.726	0.638	—
No. id	—	21	21
AR1	—	—	−1.62 (0.105)
AR2	—	—	−1.26 (0.209)
Sargan test	—	—	646.50 (0.000)

Note: ***, **, and * show the significance level at 1, 5, and 10 percent, respectively. Data source: BP statistics and WDI.

governments of these developing countries should take measures to diversify energy supply to meet demand and promote and attract foreign investors to provide funds and technologies for green production.

The results on the impact of financial development on carbon emission are also significant and positive, which indicates its increase in emission in the sample countries. This result also matches Table 4 results. For instance, the GMM system model shows that a percent increase in financial development increases carbon emission by 0.08 percent in the sample countries.

Urban population is also positive and significant which also increases carbon emission, while labor forces are negative. Its means that a percentage change in the labor force reduces the carbon emissions of developing countries by 0.9 percent.

Table 8: Summary of results.

Variables	RE	RE sources	Variables	NRE	NRE sources
RE	−sign	—	NRE	+sig	—
HDR	—	−sign	CL	—	+sig
SLR	—	−sign	NG	—	+sig
WND	—	+sig	OL	—	+sig
FD	+sig	+sig	FD	+sig	+sig
UP	+sig	+sig	UP	+sig	−sig
LF	−sig	−sig	LF	−sig	−sig

Note: +sig and −sig show positive and negative significant, respectively.

5. Conclusion and Policy Implication

This study uses data from 21 developing countries downloaded from WDI and BP statistics from 1970 to 2018 to examine the impact of energy consumption on carbon emissions. By adopting the OLS model and fixed effects and dynamic system GMM, the research results show the significant negative effect of renewable energy and its sources on carbon emissions means that it has improved the environmental quality of 21 developing countries. On the contrary, in Model 2 and Model 4, the impact of nonrenewable energy and its sources, including oil, natural gas, and coal, has a positive impact on carbon emissions, indicating that it has an increasing impact on carbon emissions in developing countries and the environmental quality has declined. It is found in all models that financial development is positive, which indicates that financial development will increase carbon emissions. The results of various indicators are summarized in Table 8, showing the positive and negative impacts of indicators on carbon emissions.

The results of the survey guide countries to formulate policies to reduce carbon emissions by reducing the use of fossil fuel energy sources such as coal, oil, and natural gas, as this will increase carbon dioxide emissions and to develop technologies that may help reduce environmental impact. Since our research sample is a developing country rather than a developed country, they may still use fossil fuels such as coal, oil, and natural gas to meet the more environmentally unfavorable energy needs, but compared to coal, it may be better to use natural gas because compared with coal, natural gas consumption may not be too harmful. The economic growth of these countries may not be conducive to financing renewable energy projects to obtain renewable energy, so it can be suggested that natural gas may be better than coal consumption, but in the future, these countries should strive to promote economic growth and invest in renewable energy to avoid the use of nonrenewable energy sources, such as coal and natural gas.

The governments of these developing countries must call for high-level initiatives to diversify energy supply to meet growing demand of energy and promote the attraction of foreign investors who provide green production technologies and capital. By doing so, renewable energy will be used, which will help reduce emissions and help promote economic growth. In developing countries, nonrenewable energy is used as fuel for industrial production and household consumption. Therefore, it is recommended to switch to renewable energy sources that have minimal or no environmental impact. Policy makers should adopt policies and encourage environmentally-friendly equipment, vehicles, and utilization to minimize environmental degradation in developing countries. The use of nonrenewable energy is harmful to the quality of the environment, and developing countries use this energy to promote economic activities that lead to carbon emissions and environmental degradation. Obviously, developing countries continue to focus on promoting economic growth. They are using energy to increase production and promote economic growth, and the use of energy consumption has increased the level of carbon emissions in these countries. Compared with the environmental quality of developed countries, developing countries have more serious pollution.

Most researchers found that the degree of environmental degradation in developed countries is low because these countries use renewable energy and the quality of institutions in these countries is better. This is also the reason for the harmful effects of environmental quality protection and other factors on environmental quality if they use nonrenewable energy. Our research results conclude that nonrenewable energy is mainly used in developing countries to promote economic growth. At the same time, we also believe that this effect may be different in different countries such as developing and developed countries. For developing countries, while focusing on promoting economic growth, it is important not to ignore the environmental impact of using nonrenewable resources. In the future, research on the same topic should be conducted on different samples to compare these findings. Future research may also include institutional quality variables and test environmental Kuznets curve. Developing countries focus on improving economic growth by using nonrenewable energy to understand whether economic growth will improve environmental quality when income reaches a certain level.

Data Availability

The data used in this article can be obtained from the World Bank World Development Indicators and BP Statistics. The WDI link is https://databank.worldbank.org/source/world-development-indicators.

Conflicts of Interest

The authors declare that there are no conflicts of interest regarding the publication of this article.

References

[1] H. M. A. Siddique and M. T. Majeed, "Energy consumption, economic growth, trade and financial development nexus in South Asia," *Pakistan Journal of Commerce and Social Sciences (PJCSS)*, vol. 9, no. 2, pp. 658–682, 2015.

[2] H. M. A. Siddique, "Impact of financial development and energy consumption on CO_2 emissions: evidence from Pakistan," *Bulletin of Business and Economics*, vol. 6, no. 2, pp. 68–73, 2017.

[3] Y. Wolde-Rufael and K. Menyah, "Nuclear energy consumption and economic growth in nine developed countries," *Energy Economics*, vol. 32, no. 3, pp. 550–556, 2010.

[4] A. K. Akella, R. P. Saini, and M. P. Sharma, "Social, economical and environmental impacts of renewable energy systems," *Renewable Energy*, vol. 34, no. 2, pp. 390–396, 2009.

[5] F. Bilgili, E. Koçak, and Ü. Bulut, "The dynamic impact of renewable energy consumption on CO_2 emissions: a revisited Environmental Kuznets Curve approach," *Renewable and Sustainable Energy Reviews*, vol. 54, pp. 838–845, 2016.

[6] M. B. Jebli and S. B. Youssef, "Renewable energy consumption and agriculture: evidence for cointegration and Granger causality for Tunisian economy," *The International Journal of Sustainable Development and World Ecology*, vol. 24, no. 2, pp. 149–158, 2017.

[7] D. Balsalobre-Lorente, M. Shahbaz, D. Roubaud, and S. Farhani, "How economic growth, renewable electricity and natural resources contribute to CO_2 emissions?" *Energy Policy*, vol. 113, pp. 356–367, 2018.

[8] E. Dogan and I. Ozturk, "The influence of renewable and non-renewable energy consumption and real income on CO_2 emissions in the USA: evidence from structural break tests," *Environmental Science and Pollution Research*, vol. 24, no. 11, pp. 10846–10854, 2017.

[9] K. Ito, "CO_2 emissions, renewable and non-renewable energy consumption, and economic growth: evidence from panel data for developing countries," *International Economics*, vol. 151, pp. 1–6, 2017.

[10] M. Kahia, M. B. Jebli, and M. Belloumi, "Analysis of the impact of renewable energy consumption and economic growth on carbon dioxide emissions in 12 MENA countries," *Clean Technologies and Environmental Policy*, vol. 21, no. 4, pp. 871–885, 2019.

[11] H. Khan, I. Khan, and T. T. Binh, "The heterogeneity of renewable energy consumption, carbon emission and financial development in the globe: a panel quantile regression approach," *Energy Report*, vol. 6, pp. 859–867, 2020.

[12] B. Saboori and J. Sulaiman, "Environmental degradation, economic growth and energy consumption: evidence of the environmental Kuznets curve in Malaysia," *Energy Policy*, vol. 60, pp. 892–905, 2013.

[13] A. Sharif, S. A. Raza, I. Ozturk, and S. Afshan, "The dynamic relationship of renewable and nonrenewable energy consumption with carbon emission: a global study with the application of heterogeneous panel estimations," *Renewable Energy*, vol. 133, pp. 685–691, 2019.

[14] N. Apergis and J. E. Payne, "Renewable energy, output, carbon dioxide emissions, and oil prices: evidence from South America," *Energy Sources, Part B: Economics, Planning, and Policy*, vol. 10, no. 3, pp. 281–287, 2015.

[15] G. Bölük and M. Mert, "Fossil & renewable energy consumption, GHGs (greenhouse gases) and economic growth: evidence from a panel of EU (European Union) countries," *Energy*, vol. 74, pp. 439–446, 2014.

[16] M. B. Jebli and S. B. Youssef, "The role of renewable energy and agriculture in reducing CO_2 emissions: evidence for North Africa countries," *Ecological Indicators*, vol. 74, pp. 295–301, 2017.

[17] U. Al-Mulali, I. Ozturk, and H. H. Lean, "The influence of economic growth, urbanization, trade openness, financial development, and renewable energy on pollution in Europe," *Natural Hazards*, vol. 79, no. 1, pp. 621–644, 2015.

[18] S. A. H. Zaidi, Danish, F. Hou, and F. M. Mirza, "The role of renewable and non-renewable energy consumption in CO_2 emissions: a disaggregate analysis of Pakistan," *Environmental Science and Pollution Research*, vol. 25, no. 31, pp. 31616–31629, 2018.

[19] I. Hanif, "Impact of economic growth, nonrenewable and renewable energy consumption, and urbanization on carbon emissions in Sub-Saharan Africa," *Environmental Science and Pollution Research*, vol. 25, no. 15, pp. 15057–15067, 2018.

[20] O. B. Awodumi and A. O. Adewuyi, "The role of non-renewable energy consumption in economic growth and carbon emission: evidence from oil producing economies in Africa," *Energy Strategy Reviews*, vol. 27, Article ID 100434, 2020.

[21] M. K. Khan, M. I. Khan, and M. Rehan, "The relationship between energy consumption, economic growth and carbon dioxide emissions in Pakistan," *Financial Innovation*, vol. 6, no. 1, pp. 1–13, 2020.

[22] C. Işık, S. Ongan, and D. Özdemir, "Testing the EKC hypothesis for ten US states: an application of heterogeneous panel estimation method," *Environmental Science and Pollution Research International*, vol. 26, no. 11, pp. 10846–10853, 2019.

[23] M. K. Anser, I. Hanif, M. Alharthi, and I. S. Chaudhry, "Impact of fossil fuels, renewable energy consumption and industrial growth on carbon emissions in Latin American and Caribbean economies," *Atmósfera*, vol. 33, no. 3, pp. 201–213, 2020.

[24] W. Zhao, R. Zhong, S. Sohail, M. T. Majeed, and S. Ullah, "Geopolitical risks, energy consumption, and CO_2 emissions in BRICS: an asymmetric analysis," *Environmental Science and Pollution Research*, vol. 28, pp. 39668–39679, 2021.

[25] M. S. Karimi, S. Ahmad, H. Karamelikli et al., "Dynamic linkages between renewable energy, carbon emissions and economic growth through nonlinear ARDL approach: evidence from Iran," *PLoS One*, vol. 16, no. 7, Article ID e0253464, 2021.

[26] L. Yuping, M. Ramzan, L. Xincheng et al., "Determinants of carbon emissions in Argentina: the roles of renewable energy consumption and globalization," *Energy Report*, vol. 7, pp. 4747–4760, 2021.

[27] M. T. Majeed and T. Luni, "Renewable energy, water, and environmental degradation: a global panel data approach," *Pakistan Journal of Commerce and Social Sciences (PJCSS)*, vol. 13, no. 3, pp. 749–778, 2019.

[28] H. Khan, L. Weili, I. Khan, and S. Khamphengxay, "Renewable energy consumption, trade openness, and environmental degradation: a panel data analysis of developing and developed countries," *Mathematical Problems in Engineering*, vol. 2021, Article ID 6691046, 2021.

[29] R. Inglesi-Lotz and E. Dogan, "The role of renewable versus non-renewable energy to the level of CO_2 emissions a panel analysis of sub- Saharan Africa's big 10 electricity generators," *Renewable Energy*, vol. 123, pp. 36–43, 2018.

[30] H. Ali, H. M. A. Siddique, K. Ullah, and M. T. Mahmood, "Human capital and economic growth nexus in Pakistan: the role of foreign aid," *Bulletin of Business and Economics*, vol. 7, no. 1, pp. 13–21, 2018.

[31] H. Alqaralleh, "On the nexus of CO_2 emissions and renewable and nonrenewable energy consumption in Europe: a new insight from panel smooth transition," *Energy & Environment*, vol. 32, no. 3, pp. 443–457, 2021.

[32] T. Fatima, U. Shahzad, and L. Cui, "Renewable and nonrenewable energy consumption, trade and CO_2 emissions in high emitter countries: does the income level matter?" *Journal of Environmental Planning and Management*, vol. 64, no. 7, pp. 1227–1251, 2021.

[33] R. L. Ibrahim and K. B. Ajide, "Disaggregated environmental impacts of non-renewable energy and trade openness in selected G-20 countries: the conditioning role of technological innovation," *Environmental Science and Pollution Research*, pp. 1–15, 2021.

[34] R. Sharma, M. Shahbaz, A. Sinha, and X. V. Vo, "Examining the temporal impact of stock market development on carbon intensity: evidence from South Asian countries," *Journal of Environmental Management*, vol. 297, Article ID 113248, 2021.

[35] Q. Fu, S. Álvarez-Otero, M. S. Sial et al., "Impact of renewable energy on economic growth and CO2 emissions-evidence from BRICS countries," *Processes*, vol. 9, no. 8, p. 1281, 2021.

[36] F. Kula, "The long-run relationship between renewable electricity consumption and GDP: evidence from panel data," *Energy Sources, Part B: Economics, Planning, and Policy*, vol. 9, no. 2, pp. 156–160, 2014.

[37] L. Charfeddine and M. Kahia, "Impact of renewable energy consumption and financial development on CO_2 emissions and economic growth in the MENA region: a panel vector autoregressive (PVAR) analysis," *Renewable Energy*, vol. 139, pp. 198–213, 2019.

[38] A. O. Adewuyi and O. B. Awodumi, "Renewable and non-renewable energy-growth-emissions linkages: review of emerging trends with policy implications," *Renewable and Sustainable Energy Reviews*, vol. 69, pp. 275–291, 2017.

[39] R. Inglesi-Lotz, "The impact of renewable energy consumption to economic growth: a panel data application," *Energy Economics*, vol. 53, pp. 58–63, 2016.

[40] S. Cho, E. Heo, and J. Kim, "Causal relationship between renewable energy consumption and economic growth: comparison between developed and less-developed countries," *Geosystem Engineering*, vol. 18, no. 6, pp. 284–291, 2015.

[41] E. Dogan, "The relationship between economic growth and electricity consumption from renewable and non-renewable sources: a study of Turkey," *Renewable and Sustainable Energy Reviews*, vol. 52, pp. 534–546, 2015.

[42] M. Shahbaz, N. Loganathan, M. Zeshan, and K. Zaman, "Does renewable energy consumption add in economic growth? An application of auto-regressive distributed lag model in Pakistan," *Renewable and Sustainable Energy Reviews*, vol. 44, pp. 576–585, 2015.

[43] H. Khan, I. Khan, L. T. Kim Oanh, and Z. Lin, "The dynamic interrelationship of environmental factors and foreign direct investment: dynamic panel data analysis and new evidence from the globe," *Mathematical Problems in Engineering*, vol. 2020, Article ID 2812489, 12 pages, 2020.

[44] H. Khan, M. S. Jan, J. Hu, and C. I. Khan, "Impact of governance on foreign direct investment in context of Pakistan," *Journal of International Finance and Economics*, vol. 19, no. 1, pp. 53–64, 2019.

[45] M. Cetin, E. Ecevit, and A. G. Yucel, "The impact of economic growth, energy consumption, trade openness, and financial development on carbon emissions: empirical evidence from Turkey," *Environmental Science and Pollution Research*, vol. 25, no. 36, pp. 36589–36603, 2018.

[46] H. Khan, L. Weili, and I. Khan, "Environmental innovation, trade openness and quality institutions: an integrated investigation about environmental sustainability," *Environment, Development and Sustainability*, pp. 1–31, 2021.

[47] J. A. Bhat, "Renewable and non-renewable energy consumption-impact on economic growth and CO_2 emissions in five emerging market economies," *Environmental Science and Pollution Research*, vol. 25, no. 35, pp. 35515–35530, 2018.

[48] H. Khan, L. Weili, I. Khan, and L. T. Kim Oanh, "Recent advances in energy usage and environmental degradation: does quality institutions matter? a worldwide evidence," *Energy Report*, vol. 7, pp. 1091–1103, 2021.

[49] Blundell, R., & Bond, S. (1995). On the Use of Initial Conditions in Dynamic Panel Data Models. Retrieved from.

[50] R. Blundell and S. Bond, "Initial conditions and moment restrictions in dynamic panel data models," *Journal of Econometrics*, vol. 87, no. 1, pp. 115–143, 1998.

[51] M. A. Boutabba, "The impact of financial development, income, energy and trade on carbon emissions: evidence from the Indian economy," *Economic Modelling*, vol. 40, pp. 33–41, 2014.

[52] E. Dogan and F. Seker, "The influence of real output, renewable and non-renewable energy, trade and financial development on carbon emissions in the top renewable energy countries," *Renewable and Sustainable Energy Reviews*, vol. 60, pp. 1074–1085, 2016.

[53] A. Jalil and M. Feridun, "The impact of growth, energy and financial development on the environment in China: a cointegration analysis," *Energy Economics*, vol. 33, no. 2, pp. 284–291, 2011.

[54] T.-H. Le, "Dynamics between energy, output, openness and financial development in sub-Saharan African countries," *Applied Economics*, vol. 48, no. 10, pp. 914–933, 2016.

[55] I. Ozturk and A. Acaravci, "The long-run and causal analysis of energy, growth, openness and financial development on carbon emissions in Turkey," *Energy Economics*, vol. 36, pp. 262–267, 2013.

[56] M. Shahbaz, Z. Mushtaq, F. Andaz, and A. Masood, "Does proline application ameliorate adverse effects of salt stress on growth, ions and photosynthetic ability of eggplant (Solanum melongena L.)?" *Scientia Horticulturae*, vol. 164, pp. 507–511, 2013.

[57] P. Poumanyvong and S. Kaneko, "Does urbanization lead to less energy use and lower CO_2 emissions? a cross-country analysis," *Ecological Economics*, vol. 70, no. 2, pp. 434–444, 2010.

[58] A. Rauf, X. Liu, W. Amin et al., "Does sustainable growth, energy consumption and environment challenges matter for Belt and Road Initiative feat? a novel empirical investigation," *Journal of Cleaner Production*, vol. 262, Article ID 121344, 2020.

[59] M. W. Ahmad, M. Mourshed, D. Mundow, M. Sisinni, and Y. Rezgui, "Building energy metering and environmental monitoring - a state-of-the-art review and directions for future research," *Energy and Buildings*, vol. 120, pp. 85–102, 2016.

[60] O. Mohiuddin, S. Asumadu-Sarkodie, and M. Obaidullah, "The relationship between carbon dioxide emissions, energy consumption, and GDP: a recent evidence from Pakistan," *Cogent Engineering*, vol. 3, no. 1, Article ID 1210491, 2016.

[61] K. Alkhathlan and M. Javid, "Carbon emissions and oil consumption in Saudi Arabia," *Renewable and Sustainable Energy Reviews*, vol. 48, pp. 105–111, 2015.

[62] M. B. Jebli, S. B. Youssef, and I. Ozturk, "Testing environmental Kuznets curve hypothesis: the role of renewable and non-renewable energy consumption and trade in OECD countries," *Ecological Indicators*, vol. 60, pp. 824–831, 2016.

[63] M. Shahbaz, G. S. Uddin, I. U. Rehman, and K. Imran, "Industrialization, electricity consumption and CO_2 emissions in Bangladesh," *Renewable and Sustainable Energy Reviews*, vol. 31, pp. 575–586, 2014.

[64] S. Farhani and M. Shahbaz, "What role of renewable and non-renewable electricity consumption and output is needed to initially mitigate CO_2 emissions in MENA region?" *Renewable and Sustainable Energy Reviews*, vol. 40, pp. 80–90, 2014.

[65] Danish and Z. Wang, "Dynamic relationship between tourism, economic growth, and environmental quality," *Journal of Sustainable Tourism*, vol. 26, no. 11, pp. 1928–1943, 2018.

Hindawi
Mathematical Problems in Engineering
Volume 2021, Article ID 9934887, 10 pages
https://doi.org/10.1155/2021/9934887

Research Article

Nonlinear Variable Resistor-Based FCL for Fault Ride-Through Performance Enhancement of DFIG-Based Wind Turbines

Mehdi Firouzi,[1] **Mohammadreza Shafiee**,[2] **and Mojtaba Nasiri**[3]

[1]*Department of Electrical Engineering, Abhar Branch, Islamic Azad University, Abhar, Iran*
[2]*Department of Electrical and Computer Engineering, University of Semnan, Semnan, Iran*
[3]*Solar Energy Applications Group, School of Engineering, Trinity College Dublin, Dublin 2, Ireland*

Correspondence should be addressed to Mehdi Firouzi; paper_mehdi12@yahoo.com

Received 2 April 2021; Revised 2 June 2021; Accepted 8 June 2021; Published 18 June 2021

Academic Editor: Francesco Riganti-Fulginei

Fault ride-through (FRT) requirement is a matter of great concern for doubly fed induction generator (DFIG-) based wind turbines (WTs). This study presents a nonlinear variable resistor- (NVR-) based bridge-type fault current limiter (BFCL) to augment the FRT performance of DFIG-based WTs. First, the BFCL operation and nonlinear control design consideration of the proposed NVR-based BFCL are presented. Then, the NVR-BFCL performance is validated through simulation in PSCAD/EMTDC software. In addition, the NVR-based BFCL performance is compared with the fixed resistor- (FR-) based BFCL for a three-phase symmetrical short circuit fault at the grid side. Simulation results reveal that the NVR-based BFCL provides a smooth and effective FRT scheme and outperforms the FR-based BFCL.

1. Introduction

Increasing the connection of wind turbines (WTs) impose the adverse effects on the grid reliability and stability, especially under voltage sag conditions. Generally, WTs are classified into fixed speed and variable speed. The variable speed WTs are widely used because of variable speed operation. They include the doubly fed induction generator (DFIG) and permanent magnet synchronous generator (PMSG) [1]. For all of them, even a shallow voltage dip can cause malfunction and operation failure [2]. To ensure secure operation of grid and tackle these problems, grid operators have created new requirements as grid codes. The fault ride-through (FRT) is the main requirement of them for grid connection of WTs. It is the given major focus due to the increasing grid penetration level of wind power. Based on this, WTs must stay connected to grid under grid voltage sag [3]. Compliance with the FRT requirement of WTs differs according to wind generator technology used in them. Recently, DFIG-based WTs are getting more attention due to having partial capacity power converters, in which their ratings are 25–30% of the total rated generator, capability to control both active and reactive powers, power point tracking at variable speed, and low weight and cost compared to the PMSG [4]. However, it is vulnerable to grid voltage sag because the DFIG stator is directly connected to the grid [5].

In literature, different schemes based on software and hardware solutions [6] have been suggested and documented. The software solutions are based on the improved or changed control system of the DFIG converters with less cost [7, 8]. However, they are just suitable for handling low voltage sag conditions and cannot ride through sever voltage sag conditions, just relay on the software schemes, and require the hardware protection scheme under this condition [9]. Different types of hardware schemes such as the multistep series braking resistor (MSSBR) [10], reactive power compensators [11], DC link chopper [12], crowbar system [13], series compensators such as dynamic-voltage restorer (DVR) [14] and unified interphase power-controller (UIPC) [15], superconducting magnet energy storage (SMES) [16], and different types fault current limiters (FCLs) [17–19] are presented and reported in literature.

Generally, voltage sags in grid are mainly due to occurring short circuit faults in grid [20, 21]. Therefore, researchers are studying on mitigating the adverse effects of grid faults on WTs by using FCLs to enhance the FRT performance of WTs [22, 23]. Therefore, the installation of FCLs is receiving more attention to increase the FRT capability of WTs [24, 25].

Regarding using FCLs to increase the FRT capability of the DFIG, studies focus on bridge-type FCLs (BFCLs) and superconducting-type FCLs (SFCLs) [26]. In [27], resistive SFCL (RSFCL) is utilized for enhancing the FRT capability of the DFIG. In [28], the RSFCL is employed in the terminal of rotor windings of the DFIG to protect the rotor-side converter (RSC) from spike overcurrent and the DC-link transient overvoltage under voltage sag condition. In [29, 30], the active-type and flux-coupling-type SFCLs are used to connect the DFIG to grid and limit the transient fluctuations, respectively. In [31], the different locations of flux-coupling SFCL influence mechanism are analyzed on the DFIG FRT performance. In [32], two voltage booster schemes include DVR scheme, and resistive-type SFCL schemes are compared in terms of FRT capability of DFIGs. Simulation results show that both schemes provide fast voltage sag mitigation, which improves the FRT performance of the DFIG. In [33], a combined protection scheme includes an inductive-type SFCL, and the modified grid side converter (GSC) control system is proposed to ride through the DFIG performance. In this approach, the GSC of the DFIG supply dynamic reactive to support the grid connecting voltage. Implementation of inductive-type SFCL and simultaneous transient voltage control can smooth the recovery process of grid coupling voltage after a fault time.

The research results confirm that the application of SFCLs in different structures offers a promising interface for enhancing the FRT and facilities the integration of DFIG-based WTs to grid. But this solution requires a high manufacture cost and cooling system. In [34], the BFCL is employed in wind farm for the first time to enhance the FRT performance. In this BFCL, the bypass resistor is located in the DC side of the bridge circuit. In [35], scholars use the BFCL with a bypass resistor in the AC side to enhance the transient stability of the DFIG. From this view point, different configuration and control systems from the one presented in [34] have been developed and reported. In [36], a fuzzy-logic controller is implemented to a parallel-resonance BFCL to augment transient stability of the DFIG. In [37], a capacitor-based BFCL with capability of reactive power compensation has been proposed. In [38], a fuzzy logic controller, which is optimized by the genetic algorithm, is designed to implement the capacitor-based BFCL for enhancing the transient stability of DFIG-based wind farm. In [39], a dynamic multicell FCL (MCFCL) is presented to compensate the wind farm coupling voltage for three low, medium, and severe voltage sag conditions. It inserts the suitable number of cells in fault path to provide smooth FRT performance under whole voltage sag conditions.

On the other hand, the power system has inherently nonlinear characteristics and connection of WTs including nonlinear power electronics based converters that increase this characteristic. As a result, utilization of nonlinear controllers has better performance under grid disturbances [38, 40]. It is worthy to state that, there are a few studies regarding implementation of a control system to the BFCL for enhancing a DFIG performance under fault condition.

Considering this background, this study presents a simple nonlinear variable resistor-based BFCL (NVR-BFCL) to provide the smooth FRT under voltage sag condition. To realize this objective, a simple nonlinear control based on active power deviation is designed and implemented into the BFCL circuit to generate the nonlinear variable resister under fault condition. The efficiency of the NVR-BFCL is checked through extensive time domain simulation and performance comparison of the FR-based BFCL under 3-phase symmetrical short circuit faults. Simulation studies have been performed in PSCAD/EMTDC software environment.

2. DFIG-Based WT Model

The schematic diagram of a grid-connected DFIG-based wind turbine is illustrated in Figure 1. The induction generator, wind turbine, drive train system, and the control system of DFIG converters are the main components of the wind generation system, which are modeled as follows.

2.1. Aerodynamic Modeling of WT. To model the wind turbine in PSCAD/EMTDC software, there are two models such as MODE 2 and MODE 5 in master library of this software. In this work, to model the wind turbine, the MODE 2 is utilized, in which the mechanical power (P_m) extracted from wind power is given by the following equation [37]:

$$P_m = 0.5\pi\rho R^2 C_p(\lambda,\beta)V_W^3. \tag{1}$$

In (1), ρ introduces the air density, and R and V_w are the blades radius and wind speed, respectively. C_p in (1) is determined based on tip speed ratio (λ) and pitch angle (β) and is known as power coefficient. It is determined as

$$C_p(\lambda,\beta) = 0.22\left(\frac{116}{\lambda_c} - 0.4\beta - 5\right)e^{-12.5\lambda_c},$$
$$\lambda_c = \frac{1}{\left((1/\lambda + 0.08\beta) - \left(0.035/\beta^3 - 1\right)\right)}. \tag{2}$$

In the MODE 2 wind turbine used in this work, the drive train system is presented by the common two-mass model. The schematic diagram of this model is shown in Figure 2, and related equations of this model are given by the following equation.

$$\begin{bmatrix} \dot{\omega}_g \\ \dot{\omega}_t \\ \dot{\delta}_{tg} \end{bmatrix} = \begin{bmatrix} \frac{D_{tg}}{2H_g} & \frac{-D_{tg}}{2H_g} & \frac{K_{tg}}{2H_g} \\ \frac{D_{tg}}{2H_t} & \frac{-D_{tg}}{2H_t} & \frac{-K_{tg}}{2H_t} \\ -1 & 1 & 0 \end{bmatrix} \begin{bmatrix} \omega_g \\ \omega_t \\ \delta_{tg} \end{bmatrix} + \begin{bmatrix} \frac{-1}{2H_g} & 0 & 0 \\ 0 & \frac{1}{2H_t} & 0 \\ 0 & 0 & 0 \end{bmatrix} \begin{bmatrix} T_g \\ T_t \\ 0 \end{bmatrix}. \tag{3}$$

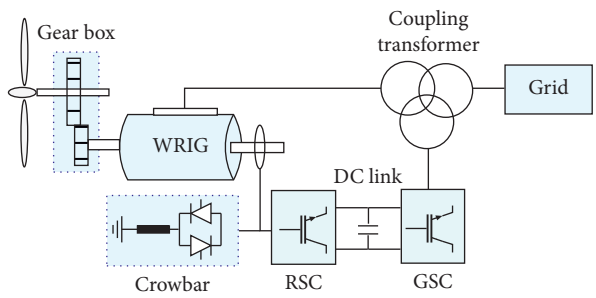

Figure 1: DFIG-based WT.

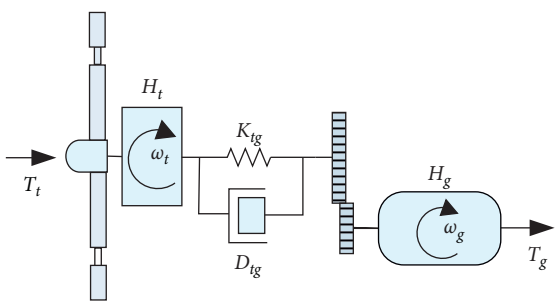

Figure 2: Two-mass model.

2.2. DFIG Model and Control System. The DFIG is composed of a wounded rotor IG, a RSC connected to the GSC by a DC link capacitor, and a WT, as shown in Figure 1. The equivalent power circuit of the DFIG in $d-q$ reference frame is shown in Figure 3. According to this figure, the stator and rotor voltage and flux equations are written as follows:

$$\begin{aligned} V_{dqs} &= R_s\, i_{dqs} + \frac{\mathrm{d}\lambda_{dqs}}{\mathrm{d}t} - \omega_s \lambda_{dqs}, \\ V_{dqr} &= R_r\, i_{qrdqr} + \frac{\mathrm{d}\lambda_{dqr}}{\mathrm{d}t} - (\omega_s - \omega_r)\lambda_{dqr}, \\ \lambda_{dqs} &= L_s\, i_{dqs} + L_m\, i_{dqs}, \\ \lambda_{dqr} &= L_s\, i_{dqr} + L_m\, i_{dqr}. \end{aligned} \tag{4}$$

In these equations, $L_s = (L_{ls}L_m/(L_{ls}+L_m)), L_r = (L_{lr}L_m/(L_{lr}+L_m))$. i_{dqs} and i_{dqr} introduce the $d-q$ component of stator and rotor currents, respectively. $i_{\mathrm{d}qs}$ and rotor current $i_{\mathrm{d}qr}$ are the $d-q$ components of the stator and rotor currents. Considering Figure 3, the GSC dynamic equations are written as [40]

$$V_{dqs} = V_{dqg} + R_g\, i_{dqg} + L_g \frac{\mathrm{d}\lambda_{dqg}}{\mathrm{d}t} + \omega_s L_g i_{dqg}. \tag{5}$$

And also the DC link dynamic equation is expressed as

$$V_{dc} i_{dc} = P_g - P_r - P_{\mathrm{loss}}. \tag{6}$$

The DFIG active and reactive powers, i.e., P_S and Q_S are expressed as

$$\begin{aligned} P_S &= \frac{3}{2}\left(V_{qs} i_{qs} + V_{ds} i_{ds}\right) = -\frac{3}{2}\left(\frac{L_m}{L_S} V_{qs} i_{qr}\right), \\ Q_S &= \frac{3}{2}\left(V_{qs} i_{ds} - V_{ds} i_{qs}\right) = \frac{3}{2}\frac{L_m}{L_S} V_{qs}\left(i_{ms} - i_{dr}\right). \end{aligned} \tag{7}$$

The control diagram of the RSC and GSC are presented in Figure 3. The RSC regulates P_S and Q_S by controlling i_{qr} and i_{dr}, respectively. Also, the GSC regulates V_{dc} and V_{PCC} at the determined level by controlling i_{qs} and $i_{\mathrm{d}s}$, respectively. V_{dc} and V_{PCC} introduce the DC link and the PCC voltage.

3. Nonlinear Variable Resistor (NVR)-BFCL

The single-phase circuit of the NVR-based BFCL is shown in Figure 4. It includes of following elements:

(1) Bridge rectifier includes diodes D_1–D_4

(2) IGBT switch, which is represented by T

(3) DC reactor L_D suppresses the increasing rate of fault current and protects the semiconductor switches against $(\mathrm{d}i/\mathrm{d}t)$

(4) Discharging resistor (R_D) and

(5) Diode D_m in series with R to prevent inverse current due to forward voltage of IGBT switch

3.1. Principle Operation of the DBIFCL. To investigate the NVR-BFCL performance, the system shown in Figure 5 is used. Under normal operation, the AC current flow through line is converted to DC current (i_D) by the bridge rectifier circuit. It charges L_D to the peak value of line current. T is closed to bypass (R_D) for providing a low impedance path. $D_1 - L_D - r_D - D_4 - T$ and $D_2 - L_D - r_D - D_3 - T$ paths carry the line current under positive and negative half cycles of frequency, respectively. The current flowing through r_D and semiconductor switches provides some power losses and voltage drop, which is ignorable in comparison with the line voltage drop. When a fault happens at downstream of grid, the rise of line current and the rate of $(\mathrm{d}i/\mathrm{d}t)$ are limited by L_D to ensure the BFCL' safe operation and prevent instantaneous voltage drop at coupling point voltage. Then, the BFCL control system switches T to put a NVR in fault path. There are two approaches to achieve this. In approach one, when the coupling point voltage falls below the threshold value, the BFCL control system turns off the IGBT switch and inserts the total limiting resistor in fault path. In the second approach, the control system of the BFCL controls the duty cycle (D) of IGBT switching to provide a variable resistor based on the D, where D is defined as

$$D = \frac{t_{\mathrm{on}}}{T}. \tag{8}$$

T is the period of the PWM currier wave, and t_{on} represents the duration time that the T is ON for each period. In this approach, the BFCL inserts a fraction of the total limiting resistor in fault path to provide a variable resistor (R_V), which is expressed by following equation:

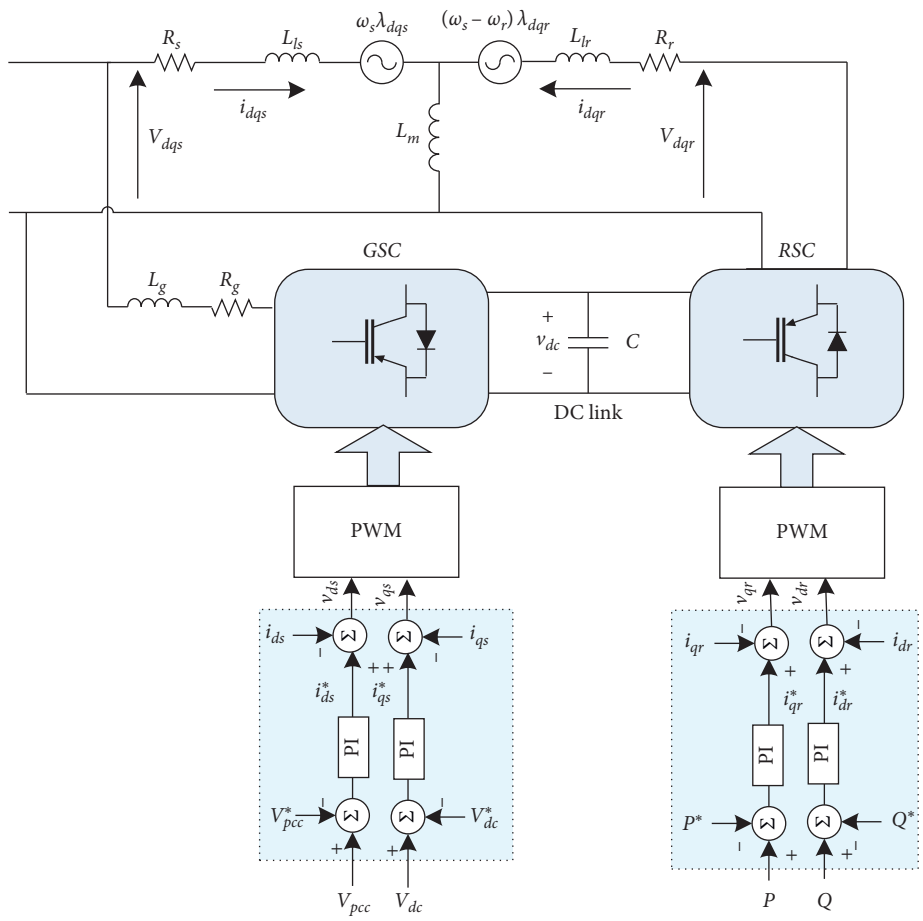

Figure 3: DFIG equivalent circuit and its converters.

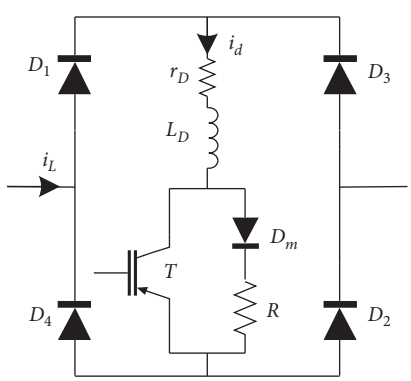

Figure 4: Power circuit of the BFCL.

$$R_V = R\,(1 - D). \tag{9}$$

In this study, the BFCL is controlled based on the second approach. Under fault condition, the BFCL control system detects the fault and implements the nonlinear control for switching T to produce a nonlinear variable resistor. To control the switching of T, the active power deviation ($\Delta P = P_G - P_T$) is used to implement the nonlinear control to provide adaptive active power-based NVR. Therefore, the faulted line short circuit current is limited, and the PCC voltage is boosted as well. Also, (R_V) dissipates the active power generated by the DFIG, which enhances the FRT capability. When the fault is cleared, the PCC voltage returns back to the prefault level and control system turns on T.

3.2. Nonlinear Control of the BFCL Resistor. To provide the NVR-based BFCL, the active power deviation ΔP is used as input to provide the duty ratio D under fault condition, which is expressed as

$$D = e^{-\left(\Delta P/T_p\right)}. \tag{10}$$

Considering (10), t_{on} is expressed as

$$t_{\text{on}} = Te^{-\left(\Delta P/T_p\right)}. \tag{11}$$

Considering (10) and (11), R_V is expressed by following equation:

$$R_V = R\left(1 - e^{-\left(\Delta P/T_p\right)}\right). \tag{12}$$

It can be seen from (12) that by implementation of a nonlinear control strategy switching, the BFCL provides a NVR as function of the active power deviation. To select a proper time constant (T_p), the active power deviations index is used. It is defined as

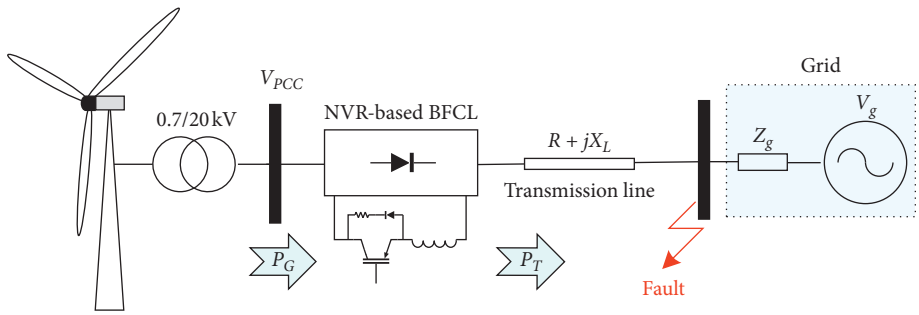

Figure 5: Test system.

$$\Delta P = \int_0^T |\Delta P| \mathrm{d}t. \tag{13}$$

Figure 6 demonstrates the active power deviation index for different values of (T_p). It can be seen that for (T_p = 1 ms), the system has better performance.

3.3. NVR-BFCL Control System. The NVR-based BFCL control flowchart is shown in Figure 7. According to this flowchart, the PCC bus voltage (V_{PCC}) is considered as control signal to detect the short circuit at the grid side. When a short circuit fault occurs in the grid side, V_{PCC} experiences a voltage sag. Once V_{PCC} becomes less than the threshold value V_T, the control circuit detects the fault. V_T considered to be 0.95 pu is considered in this work. After detection of voltage sag at PCC bus, the active power deviation ΔP is measured and is used as input to provide the duty ratio D under fault condition. Considering ΔP, the duty ratio D is determined and implemented to the IGBT switch to provide a NVR under fault condition.

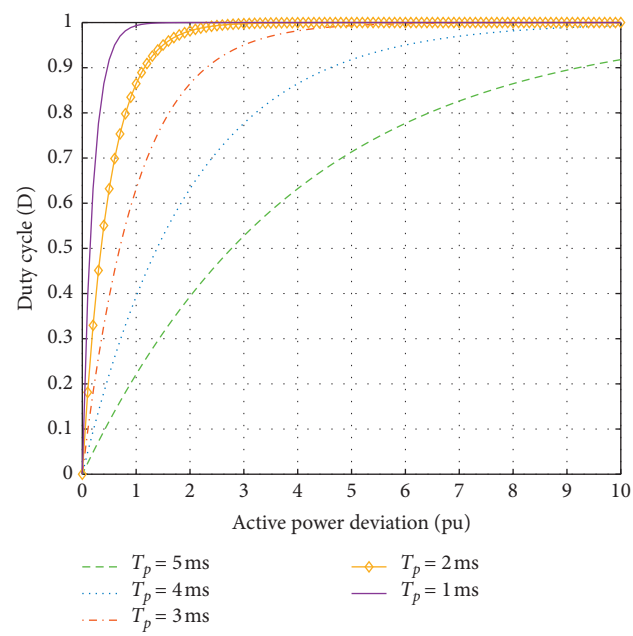

Figure 6: Nonlinear controller response.

4. Simulation Results

To assess the NVR-based BFCL performance, the system shown in Figure 5 is simulated in PSCAD/EMTDC software. In this simulation study, a three-phased short circuit fault is applied to the transmission line after the FCL location at the grid side. The fault occurs at t = 10 s. After 0.15 s, the circuit breaker isolates the fault. To FRT analysis, the wind speed is considered 14 m/s. Parameters of this system are presented in Table 1.

The simulated DFIG produce the rated nominal power at this speed. To investigate the efficiency of the NVR-based BFCL, three scenarios are simulated as follows:

Scenario A: without FCL

Scenario B: with FR-based BFCL

Scenario C: with NVR-based BFCL

Figure 8 shows the PCC voltage for all scenarios. The PCC voltage is reduced to 0.18 pu in scenario A, under fault condition. However, the NVR-based BFCL provides the lowest voltage sag during and after the fault period compared with scenario B. Also, the voltage recovery process is considerably smooth and short in scenario C. The DC link voltage response of the DFIG for 3LG fault is shown in Figure 9. According this figure, the DC link voltage has the lowest overvoltage and fluctuation during and after fault time.

Figure 10 shows the DFIG active power. It drops to zero during fault in scenario A. In scenarios B and C, the active power of DFIG is prevented from abrupt change under fault condition. But, in scenario C, the proposed BFCL by providing a NVR and insertion in fault path causes the active power fluctuation that is minimized and smoothed under fault condition.

Figure 11 shows the DFIG reactive power. It absorbs −2.5 pu reactive power from the grid in scenario A to recover the PCC voltage. However, it is effectively reduced in scenarios B and C. Also, it is lowest in the scenario C, during and after fault clearance. Figure 12 shows the rotor speed of the DFIG under all scenarios.

By using FCL in scenarios B and C, the rotor speed is limited during fault. But, the NVR-based BFCL provides lower oscillation and faster stabilization. The three-phase DFIG rotor currents are presented for all scenarios shown in Figure 13. According to this figure, the rotor current experienced two transient conditions in both end of fault time.

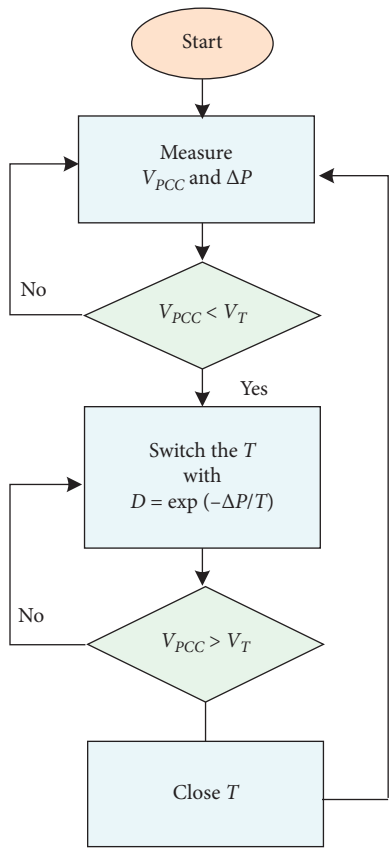

Figure 7: Control flowchart of the NVR-based BFCL.

Table 1: Study system parameters.

	Parameters	Value
Grid	Rated voltage	20 kV
	Grid frequency	50 Hz
DFIG	Rated active power	2 MW
	Rated voltage	690 V
Transmission line	Resistance	0.27 Ω/km
	Reactance	0.33 Ω/km
	Length	20 km
NVR-based BFCL	L_D	0.01 H
	r_D	1 Ω
	R	20 Ω

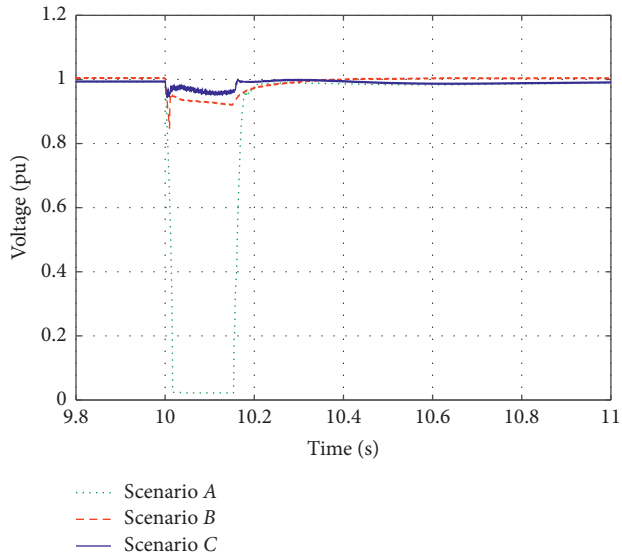

Figure 8: PCC voltage for all scenarios.

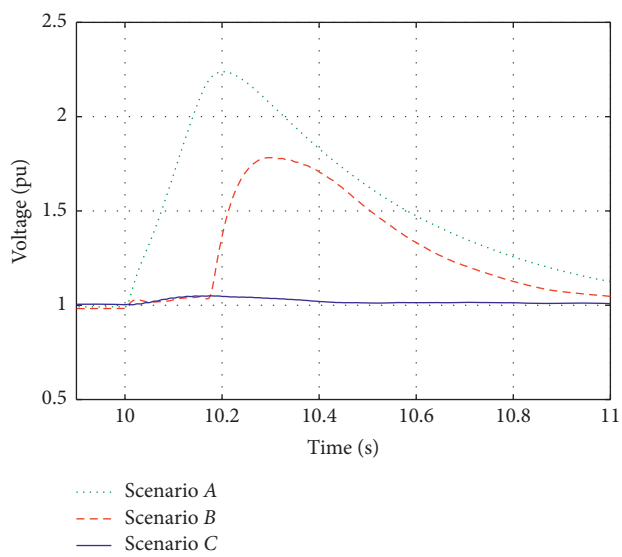

Figure 9: DFIG DC link voltage for all scenarios.

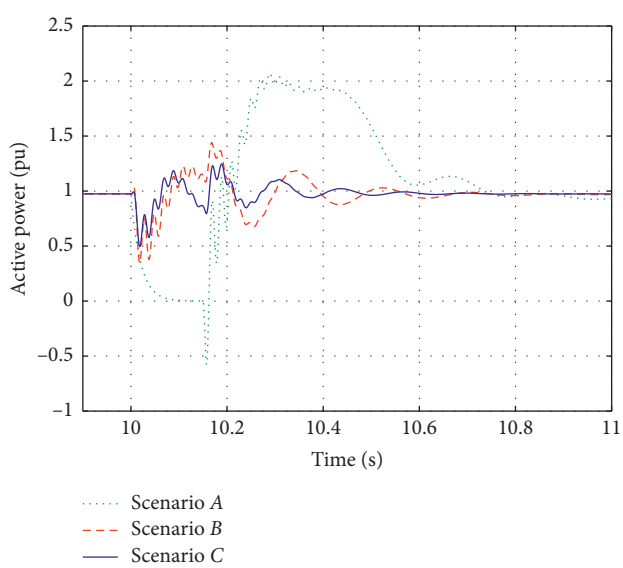

Figure 10: DFIG active power output for all scenarios.

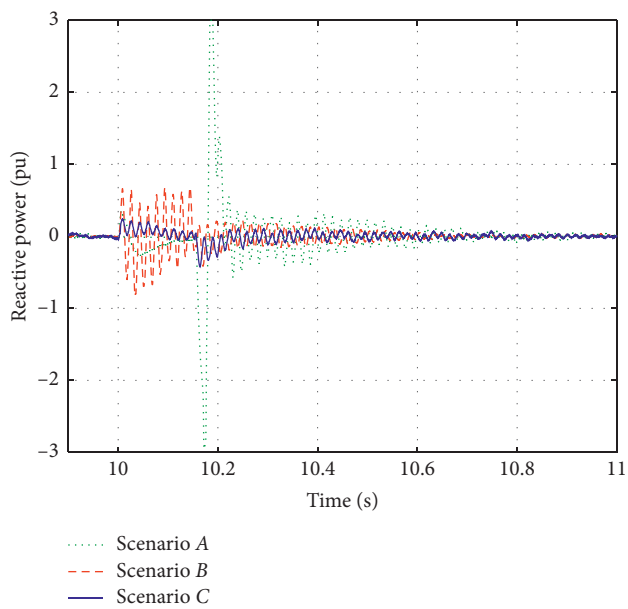

Figure 11: DFIG reactive power output for all scenarios.

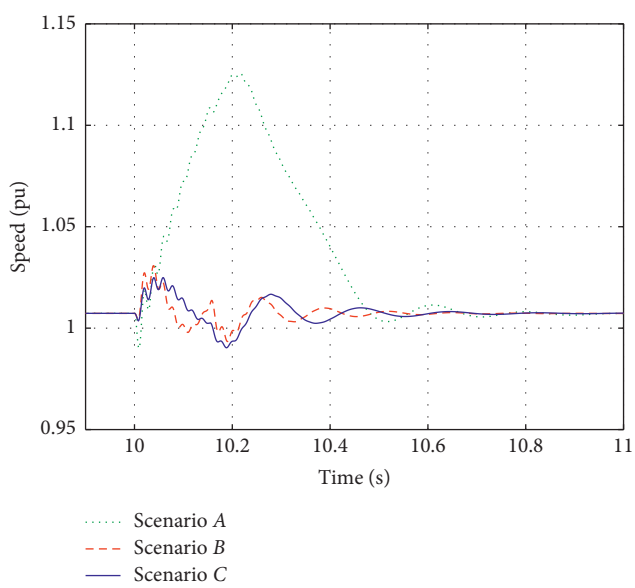

Figure 12: Rotor speed of DFIG for all scenarios.

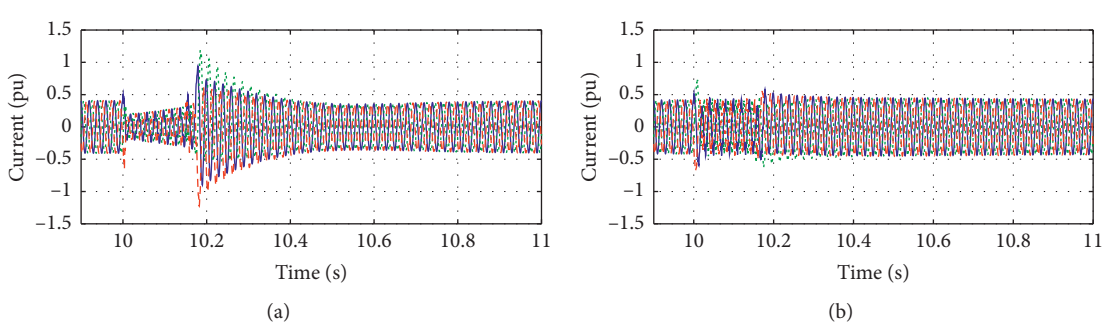

Figure 13: Continued.

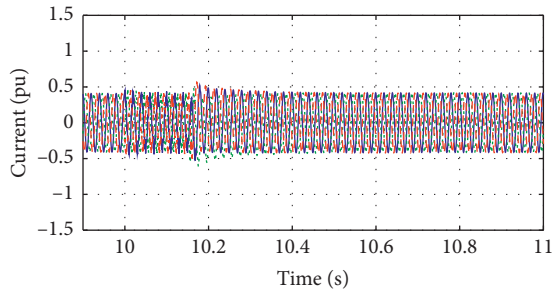

(c)

Figure 13: Rotor currents. (a) Scenario A. (b) Scenario B. (c) Scenario C.

It is increased to 2 pu at the beginning and end of fault time without using any FCL in series with WT. However, by using FCL in scenarios B and C, the transient overcurrent at both ends of fault time is restricted. However, the NVR-based BFCL provides smooth transient at both ends of fault time.

5. Conclusions

In this study, a nonlinear control system is designed and implemented to the conventional BFCL to improve the FRT capability of the DFIG-based WTs. It provides a nonlinear variable resistor (NVR), which provides a variable resistor under fault condition depending on the active power deviations during fault. Simulation results show that the NVR-based BFCL is an extremely competent scheme compared to the FR-based BFCL and has better responses in terms of voltage deviations, active power fluctuation, rotor current mitigation, and DC link overvoltage under short circuit faults.

Data Availability

There are no data availability.

Conflicts of Interest

The authors declare that they have no conflicts of interest.

References

[1] M. Liserre, R. Cardenas, M. Molinas, and J. Rodriguez, "Overview of multi-MW wind turbines and wind parks," *IEEE Transaction on Industrial Electronic*, vol. 58, no. 4, pp. 1081–1095, 2011.

[2] M. Nasiri, J. Milimonfared, and S. H. Fathi, "A review of low-voltage ride-through enhancement methods for permanent magnet synchronous generator based wind turbines," *Renewable and Sustainable Energy Reviews*, vol. 47, no. 47, pp. 399–415, 2015.

[3] M. Tsili and S. Papathanassiou, "A review of grid code technical requirements for wind farms," *IET Renewable Power Generation*, vol. 3, no. 12, pp. 308–332, 2009.

[4] A. J. Laafou, A. A. Madi, A. Addaim, and A. Intidam, "Dynamic modeling and improved control of a grid-connected DFIG used in wind energy conversion systems," *Mathematical Problems in Engineering*, vol. 2020, Article ID 1651648, , 2020.

[5] K. Okedu and H. Barghash, "Enhancing the performance of DFIG wind turbines considering excitation parameters of the insulated gate bipolar transistors and a new PLL scheme," *Frontiers in Energy Research*, vol. 8, Article ID 620277.

[6] M. J. Morshed and A. Fekih, "A new fault ride-through control for DFIG-based wind energy systems," *Electric Power System Research*, vol. 146, pp. 258–269, 2013.

[7] R. Zhu and Z. Chen, "Closure to discussion on virtual damping flux-based LVRT control for DFIG-based wind turbine," *IEEE Transactions on Energy Conversion*, vol. 31, no. 1, pp. 408-409, 2016.

[8] D. Zhu, X. Zou, L. Deng, Q. Huang, S. Zhou, and Y. Kang, "Inductance-emulating control for DFIG-based wind turbine to ride-through grid faults," *IEEE Transactions on Power Electronics*, vol. 32, no. 11, pp. 8514–8525, 2017.

[9] H. Shahbabaei Kartijkolaie, M. Radmehr, and M. Firouzi, "LVRT capability enhancement of DFIG-based wind farms by using capacitive DC reactor-type fault current limiter," *International Journal of Electrical Power & Energy Systems*, vol. 102, pp. 287–295, 2018.

[10] M. S. El Moursi, K. Goweily, J. L. Kirtley, and M. Abdel-Rahman, "Application of series voltage boosting schemes for enhanced fault ridethrough performance of fixed speed wind turbines," *IEEE Transactions on Power Delivery*, vol. 29, no. 1, pp. 61–71, 2014.

[11] L. Wang and D. N. Truong, "Stability enhancement of DFIG-based off shore wind farm fed to a multi machine using STATCOM," *IEEE Transaction on Power System*, vol. 28, no. 3, pp. 2882–2889, 2013.

[12] A. Jalilian, S. B. Naderi, M. Negnevitsky et al., "Controllable DC-link fault current limiter augmentation with DC chopper to improve fault ride-through of DFIG," *IET Renewable Power Generation*, vol. 11, no. 2, pp. 313–324, 2016.

[13] Q. Zhu and M. Ding, "Equivalent modeling of DFIG-based wind power plant considering crowbar protection," *Mathematical Problems in Engineering*, vol. 2016, p. 16, Article ID 8426492, 2016.

[14] X. Chen, L. Yan, X. Zhou, and H. Sun, "A novel DVR-ESS-embedded wind-energy conversion system," *IEEE Transactions on Sustainable Energy*, vol. 9, no. 3, 2018.

[15] M. Firouzi, G. B. Gharehpetian, and Y. Salami, "Active and reactive power control of wind farm for enhancement transient stability of multi-machine power system using UIPC," *IET Renewable Power Generation*, vol. 11, no. 8, pp. 1246–1252, 2017.

[16] M. H. Ali, M. Park, I.-K. Yu, T. Murata, and J. Tamura, "Improvement of wind-generator stability by fuzzy-logic-controlled SMES," *IEEE Transactions on Industry Applications*, vol. 45, no. 3, pp. 1045–1051, 2009.

[17] M. Firouzi, "A modified capacitive bridge-type fault current limiter (CBFCL) for LVRT performance enhancement of wind power plants," *International Transactions on Electrical Energy Systems*, vol. 28, no. 3, Article ID e2505, 2018.

[18] M. M. Moghimyan, "Series resonance fault current limiter (SRFCL) with MOV for LVRT enhancement in DFIG-based wind farms," *Electric Power Components and System*, vol. 47, no. 19-20, pp. 1841–1825.

[19] A. Heidary, H. Radmanesh, K. Rouzbehi, and H. M. Cheshmeheigi, "A Multifunction high-temperature superconductive power flow controller and fault current limiter," *IEEE Transactions on Applied Superconductivity*, vol. 30, no. 5, 2020.

[20] H. Radmanesh, S. H. Fathi, G. B. Gharehpetian, and A. Heidary, "Bridge-type solid-state fault current limiter based on AC/DC reactor," *IEEE Transactions on Power Delivery*, vol. 31, no. 1, pp. 200–209, 2016.

[21] M. Firouzi, S. Aslani, G. B. Gharehpetian, and A. Jalilvand, "Effect of superconducting fault current limiters on successful interruption of circuit breakers," in *Proceedings of the International Conference on Renewable Energies and Power Quality (ICREPQ 2012)*, Santiago de Compo stela, Spain, 28-30 March 2012.

[22] F. Tosato and S. Quaia, "Reducing voltage sags through fault current limitation," *IEEE Transactions on Power Delively*, vol. 16, no. 1, pp. 12–17, 2001.

[23] S. M. Alaraifi and M. S. El Moursi, "Hybrid HTS-FCL configuration with adaptive voltage compensation capability," *IEEE Transactions Applied Superconductivity*, vol. 24, no. 6, Article ID 5602208, 2014.

[24] Y. Salami, "Dynamic performance of wind farms with bridge-type superconducting fault current limiter in distribution grid," in *Proceedings of the 2nd International Conference on Electric Power and Energy Conversion Systems (EPECS)*, Sharjah, United Arab Emirates, 15-17 November 2011.

[25] M. Firouzi, M. Nasiri, M. Benbouzid, and G. B. Gharehpetian, "Application of multi-step bridge-type fault current limiter for fault ride-through capability enhancement of permanent magnet synchronous generator-based wind turbines," *International Transactions on Electrical Energy*, vol. 30, no. 11, Article ID e12611, 2020.

[26] M. Zolfaghari, M. Gilvanejad, and G. B. Gharehpetian, "A survey on fault current limiters: development and technical aspects," *International Journal of Electrical Power & Energy Systems*, vol. 118, Article ID 105729, 2020.

[27] P. M. Tripathi, S. S. Sahoo, and K. Chatterjee, "Enhancement of low-voltage ride through of wind energy conversion system using superconducting saturated core fault current limiter," *International Transactions on Electrical Energy Systems*, vol. 29, no. 4, pp. 1–19, 2019.

[28] Z. C. Zou, X. Y. Xiao, Y. F. Liu et al., "Integrated protection of DFIG-based wind turbine with a resistive-type SFCL under symmetrical and asymmetrical faults," *IEEE Transactions on Applied Superconductivity*, vol. 26, no. 7, Article ID 5603005, 2016.

[29] L. Lei Chen, F. Feng Zheng, C. Changhong Deng, Z. Zhe Li, and F. Fang Guo, "Fault ride-through capability improvement of DFIG-based wind turbine by employing a voltage-compensation-type Active SFCL," *Canadian Journal of Electrical and Computer Engineering*, vol. 38, no. 2, pp. 132–142, 2015.

[30] L. Chen, F. Zheng, C. Deng et al., "Application of a modified flux-coupling type superconducting fault current limiter to transient performance enhancement of micro-grid," *Physica C: Superconductivity and Its Applications*, vol. 518, pp. 144–148.

[31] L. Chen, C. Deng, F. Zheng, S. Li, Y. Liu, and Y. Liao, "Fault ride-through capability enhancement of DFIG-based wind turbine with a flux-coupling-type SFCL employed at different locations," *IEEE Transactions on Applied Superconductivity*, vol. 25, no. 3, 2014.

[32] S. Alaraifi, A. Moawwad, M. S. El Moursi, and V. Khadkikar, "Voltage booster schemes for fault ride-through enhancement of variable speed wind turbines," *IEEE Transactions on Sustainable Energy*, vol. 4, no. 4, pp. 1071–1081, 2013.

[33] K. J. Du, X. Y. Xiao, Y. Wang, Z. X. Zheng, and Ch. S. Li, "Enhancing fault ride-through capability of DFIG-based wind turbines using inductive SFCL with coordinated control," *IEEE Transactions on Applied Superconductivity*, vol. 29, no. 2, 2019.

[34] M. Firouzi and G. B. Gharehpetian, "Improving fault ride-through capability of fixed-speed wind turbine by using bridge-type fault current limiter," *IEEE Transactions on Energy Conversion*, vol. 28, no. 2, pp. 361–369, 2013.

[35] G. Rashid and M. H. Ali, "Transient stability enhancement of double fed induction machine based wind generator by bridge-type fault current limiter," *IEEE Transactions on Energy Conversion*, vol. 30, no. 3, 2015.

[36] M. R. Islam, J. Hasan, M. R. R. Shipon, M. A. H. Sadi, A. Abuhussein, and T. K. Roy, "Neuro fuzzy logic controlled parallel resonance type fault current limiter to improve the fault ride through capability of DFIG based wind farm," *IEEE Access*, vol. 8, pp. 115314–115334, 2020.

[37] M. Firouzi and G. B. Gharehpetian, "LVRT performance enhancement of DFIG-based wind farms by capacitive bridge-type fault current limiter," *IEEE Transactions on Energy Conversion*, vol. 9, no. 3, pp. 1118–1125, 2018.

[38] M. A. H. Sadi, A. AbuHussein, and M. A. Shoeb, "Transient performance improvement of power systems using fuzzy logic controlled capacitive-bridge type fault current limiter," *IEEE Transactions on Power Systems*, vol. 36, no. 1, 2021.

[39] M. R. Shafiee, H. Shahbabaei Kartijkolaie, M. Firouzi, S. Mobayen, and A. Fekih, "A dynamic multi-cell FCL to improve the fault ride through capability of DFIG-based wind farms," *Energies*, vol. 13, no. 20, 2020.

[40] M. Firouzi, M. Nasiri, S. Mobayen, and G. B. Gharehpetian, "Sliding mode controller-based BFCL for fault ride-through performance enhancement of DFIG-based wind turbines," *Complexity*, vol. 2020, Article ID 1259539, 12 pages, 2020.